



# Identification of a novel 1,2 oxazine that can induce apoptosis by targeting NF- $\kappa$ B in hepatocellular carcinoma cells



Chaithanya Somu<sup>a,1</sup>, Chakrabhavi Dhananjaya Mohan<sup>b,1</sup>, Sachin Ambekar<sup>c,1</sup>, Dukanya<sup>d</sup>, Shobith Rangappa<sup>e</sup>, CP Baburajeev<sup>c</sup>, Alexey Sukhorukov<sup>f</sup>, Srishti Mishra<sup>g</sup>, Muthu K Shanmugam<sup>g</sup>, Arunachalam Chinnathambi<sup>h</sup>, Tahani Awad Alahmadi<sup>i</sup>, Sulaiman Ali Alharbi<sup>h</sup>, Basappa<sup>c,d,\*\*</sup>, Kanchugarakoppal S. Rangappa<sup>a,\*</sup>

<sup>a</sup> Department of Studies in Chemistry, University of Mysore, Manasagangotri, Mysore 570006, India

<sup>b</sup> Department of Studies in Molecular Biology, University of Mysore, Manasagangotri, Mysore 570006, India

<sup>c</sup> Laboratory of Chemical Biology, Department of Chemistry, Bangalore University, Central College Campus, Palace Road, Bangalore 560001, India

<sup>d</sup> Laboratory of Chemical Biology, Department of Studies in Organic Chemistry, University of Mysore, Manasagangotri, Mysore 570006, India

<sup>e</sup> Adichunchanagiri Institute for Molecular Medicine, BG Nagara, Nagamangala Taluk, Mandya district-571448, India

<sup>f</sup> N.D. Zelinsky Institute of Organic Chemistry, Leninsky Prospect, Moscow 119991, Russia

<sup>g</sup> Department of Pharmacology, Yong Loo Lin School of Medicine, National University of Singapore 117600, Singapore

<sup>h</sup> Department of Botany and Microbiology, College of Science, King Saud University, Riyadh -11451, Saudi Arabia

<sup>i</sup> Department of Pediatrics, College of Medicine and King Khalid University Hospital, King Saud University Medical City, Riyadh 11461, Saudi Arabia

## ARTICLE INFO

### Article history:

Received 13 December 2019

Received in revised form 21 January 2020

Accepted 17 February 2020

### Keywords:

Oxazine

NF- $\kappa$ B

Anticancer

DNA fragmentation

## ABSTRACT

Constitutive activation of NF- $\kappa$ B is associated with proinflammatory diseases and suppression of the NF- $\kappa$ B signaling pathway has been considered as an effective therapeutic strategy in the treatment of various cancers including hepatocellular carcinoma (HCC). Herein, we report the synthesis of 1,2 oxazines and their anticancer potential. The antiproliferative studies presented 3-((4-(1H-benzo[d]imidazol-2-yl)piperidin-1-yl)methyl)-4-phenyl-4,4a,5,6,7,7a-hexahydrocyclopenta [e][1,2]oxazine(3i) as a lead cytotoxic agent against HCC cells. Flow cytometric analysis showed that 3i caused a substantial increase in the subG1 cell population. Annexin-V-FITC-PI staining showed a significant increase in the percentage of apoptotic cells on treatment with 3i. Transfection with p65 siRNA significantly reduced the 3i induced DNA fragmentation indicating that 3i may primarily mediate its proapoptotic effects by abrogating the NF- $\kappa$ B signaling. In addition, treatment of HCC cells with 3i decreased the DNA binding ability of NF- $\kappa$ B and NF- $\kappa$ B-dependent luciferase expression. Taken together, this report introduces 1,2-oxazine that potentially targets the NF- $\kappa$ B signaling pathway in HCC cells.

© 2020 Published by Elsevier B.V. This is an open access article under the CC BY-NC-ND license (<http://creativecommons.org/licenses/by-nc-nd/4.0/>).

## 1. Introduction

The nuclear factor- $\kappa$ B (NF- $\kappa$ B) signaling pathway is a key player in the maintenance of homeostasis by regulating growth, immune system, and inflammation [1–4]. The deregulation of NF- $\kappa$ B signaling results in initiation and progression of several diseases such as cancer, rheumatoid arthritis, colitis, atherosclerosis, asthma, diabetes, stroke, muscle wasting, neurodegenerative diseases and

viral infections [5–8]. NF- $\kappa$ B is a quiescent transcription factor that ubiquitously resides in the cytoplasm of all the mammalian cells. It was initially discovered by Ranjan Sen and David Baltimore in 1986 as a DNA binding protein that interacts with enhancer elements of the immunoglobulin kappa light chain gene in B cells [9–12]. Since its discovery, NF- $\kappa$ B has been recognized as a widely studied transcription factor and can regulate the expression of about 500 genes [13–16]. NF- $\kappa$ B is associated with a family of inhibitory proteins called I $\kappa$ B (I $\kappa$ B $\alpha$ /I $\kappa$ B $\beta$ /I $\kappa$ B $\epsilon$ ) in the cytoplasm of the unstimulated cell [17–20]. The presence of ligand on the membrane receptor initiates the cascade of signaling events that stimulate the phosphorylation, ubiquitylation, and degradation of I $\kappa$ B protein which leads to the relocation of NF- $\kappa$ B into the nucleus. In the nucleus, NF- $\kappa$ B binds to specific DNA elements and regulates the expression of genes that encodes apoptosis regulators (Bcl-2, Bcl-xL, Bim, IAP, XIAP, TRAF-1/2), cell adhesion molecules (CD44,

\* Corresponding author.

\*\* Corresponding author at: Laboratory of Chemical Biology, Department of Chemistry, Bangalore University, Central College Campus, Palace Road, Bangalore 560001, India.

E-mail addresses: [salundibasappa@gmail.com](mailto:salundibasappa@gmail.com) (Basappa),

[rangappaks@gmail.com](mailto:rangappaks@gmail.com) (K.S. Rangappa).

<sup>1</sup> These authors contributed equally to this work.

Fibronectin, ICAM-1, VCAM-1, NCAM, P-Selectin), cytokines (BAFF, TNF- $\alpha/\beta$ , RANTES, CXCL5/6, Trefoil factor 3), growth factors (VEGF-C, SCF, PIGF, NGF, M-CSF), and transcription regulators (Bcl-3, c-rel, HIF-1, nf $\kappa$ b1, nf $\kappa$ b2, p53, Stat5a) [21–24]. NF- $\kappa$ B modulates the expression of oncogenic genes involved in inflammation, cell growth, and survival, apoptosis and cancer progression [25]. Mounting shreds of evidence suggest that NF- $\kappa$ B is often overactivated in many tumors [26,27]. NF- $\kappa$ B has been identified as a potent tumor promoter and several chemical entities have been developed to target NF- $\kappa$ B in preclinical cancer models [28–30]. Notably, constitutive activation of NF- $\kappa$ B was found more frequently in hepatocellular carcinoma tumor tissues than its normal counterpart suggesting its role in tumorigenesis [31–33]. Therefore, NF- $\kappa$ B represents a novel and unique molecular target for therapeutic intervention against several cancers including hepatocellular carcinoma.

Oxazine derivatives have been evaluated extensively and reported to possess good anticancer potential in various preclinical tumor models [34–40]. Some of the oxazine derivatives have been reported to interfere with the NF- $\kappa$ B signaling pathway to impart their anticancer activity.  $\gamma$ - and  $\delta$ -tocotrienol conjugated oxazines significantly decreased the levels of phosphorylated NF- $\kappa$ B and I $\kappa$ B in the tumor tissues from mice [41]. In another study, 2-ethoxy-4,5-diphenyl-1,3-oxazine-6-one (EDPOO) decreased the nuclear levels of NF- $\kappa$ B in LPS-treated rat pheochromocytoma (PC12) cells [42]. In our previous study, we identified 2-((2-acetyl-6,6-dimethyl-4-phenyl-5,6-dihydro-2H-1,2-oxazin-3-yl)methyl)isoindoline-1,3-dione (API) as an inhibitor of NF- $\kappa$ B signaling pathway [37]. The structures of EDPOO and API are presented in Fig. 1. In our continued efforts to identify pharmacologically important small molecules [43–48], and to identify potent NF- $\kappa$ B inhibitor than the previously reported oxazines, we synthesized a panel of novel 1,2 oxazines and evaluated their anticancer and NF- $\kappa$ B inhibitory activities in tumor cells. Several hepatocellular carcinoma cell lines including HepG2 and HCCLM3 possess constitutive activation of NF- $\kappa$ B and we have demonstrated previously that, NF- $\kappa$ B targeting compounds display good cytotoxicity towards HepG2 and HCCLM3 cells. Therefore, we used HepG2 and HCCLM3 cells as representative cell lines to evaluate the possible NF- $\kappa$ B inhibitory effect of new oxazines.

## 2. Material and methods

All chemicals used were purchased from Sigma-Aldrich.  $^1\text{H}$  and  $^{13}\text{C}$  NMR spectra were recorded on a Bruker WH-200 (400 MHz) spectrometer in  $\text{CDCl}_3$  or  $\text{DMSO}-d_6$  as a solvent, using TMS as an internal standard and chemical shifts are expressed as ppm. Mass spectra were determined on an Agilent ESI MS and the elemental analyses were carried out using an Elemental Vario Cube CHNS rapid analyzer. The progress of the reaction was monitored using TLC pre-coated silica gel G plates. The small interfering RNA (siRNA) for NF- $\kappa$ B (sc-29410) and scrambled control (sc-37007) was obtained from Santa Cruz Biotechnology. DNA fragmentation

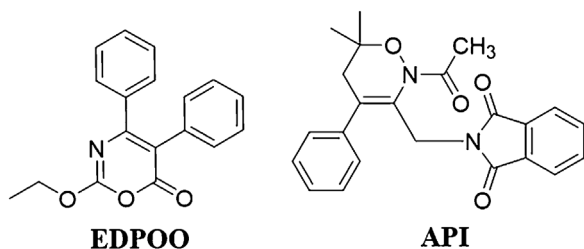


**Fig. 1.** Structures of the previously reported biologically active oxazines that target NF- $\kappa$ B.

assay kit was purchased from Roche Applied Science (CA, USA). HepG2 and MDA-MB-231 cells were previously obtained from American Type Culture Collection (ATCC) and the cells stock was maintained in our laboratory. DNA binding assay was performed using TransAM NF- $\kappa$ B Kit (ActiveMotif, USA).

## 2.1. Chemistry

### 2.1.1. Typical procedure for the synthesis of bromomethyl 1,2 oxazine derivatives (1a-f)

The synthesis of bromomethyl 1,2 oxazine derivatives was carried out as described previously [75]. In brief, the formation of 1,2-oxazine was achieved by inverse electron demand Diels–Alder reaction of nitroalkenes derived from nitroethane to olefines. The appropriate 1,2-oxazine-*N*-oxide (0.1 mol) was slowly added to a stirred solution of trimethylsilyl bromide (39.6 mL, 0.3 mol) and  $\text{Et}_3\text{N}$  (16.7 mL, 0.12 mol) in  $\text{CH}_2\text{Cl}_2$  (0.5 L) at  $-80^\circ\text{C}$ . The resulting mixture was stirred for 1 h at  $-80^\circ\text{C}$ , then MeCN (50 mL) was added and the temperature was increased to  $-30^\circ\text{C}$  within 1 h. The mixture was kept at  $-30^\circ\text{C}$  for 3 h and then diluted with EtOAc (0.5 L) and poured into a mixture of EtOAc (1.0 L) and a saturated aqueous solution of  $\text{NaHCO}_3$  (0.5 L). The aqueous phase was back-extracted with EtOAc ( $2 \times 100$  mL), and the combined organic layers were washed with  $\text{H}_2\text{O}$  ( $2 \times 100$  mL) and brine (200 mL) and dried ( $\text{Na}_2\text{SO}_4$ ). The solvents were evaporated in vacuo and the residue was filtered through a thin layer of silica gel. The obtained 3-bromomethyl-substituted 5,6-dihydro-4H-1,2-oxazines **1**, which serve as key precursors for the synthesis of new 1,2-oxazines (**3a-j**).

### 2.1.2. General procedure for the synthesis of *N*-alkylated 1,2 oxazine derivatives (3a-j)

To a solution of amines (250 mg) in 5 mL of 2-butanone,  $\text{SCS}-\text{Bi}_2\text{O}_3$  (0.8 eq), and bromomethyl 1,2 oxazine (**1a-f**) (0.1 mmol) was added and the reaction mixture was stirred at room temperature for 2 h. The progress of the reaction was monitored using thin-layer chromatography. After completion of the reaction, contents were filtered to remove the base. Subsequently, water (10 mL) was added and the product was extracted from the aqueous layer using ethyl acetate (5 mL). The extraction with ethyl acetate was repeated thrice and dried with magnesium sulfate, filtered, and concentrated in vacuum. The crude product was purified by recrystallization using ethanol.

### 2.1.3. 6-(*tert*-butyl)-8-fluoro-1-((4-(4-methoxyphenyl)-4a,5,6,7,8,8a-hexahydro-4H-benzo[e][1,2]oxazin-3-yl)methyl)-2,3-dimethylquinolin-4(1H)-one (3a)

393.2 mg (Yield 78 %); Off-white solid; mp:  $156\text{--}157^\circ\text{C}$ ; IR  $\sqrt{\text{max}}$ :  $2928.94\text{ cm}^{-1}$  ( $\nu_{\text{C-H}}$ ),  $1601.74\text{ cm}^{-1}$  ( $\nu_{\text{C=O}}$ ),  $1510.77\text{ cm}^{-1}$  ( $\nu_{\text{C-C}}$ ),  $1246.71\text{ cm}^{-1}$  ( $\nu_{\text{C-C}}$ ),  $1104.54\text{ cm}^{-1}$  ( $\nu_{\text{C-F}}$ ),  $946.45\text{ cm}^{-1}$  ( $\nu_{\text{C-O}}$ );  $^1\text{H}$  NMR ( $\text{CDCl}_3$ , 400 MHz)  $\delta$ : 7.52 (s, 1 H), 7.36–7.33 (m, 1 H), 7.11 (d,  $J = 8.4$  Hz, 2 H), 6.88 (d,  $J = 8.8$  Hz, 2 H), 4.54 (d,  $J = 10.4$  Hz, 1 H), 4.43 (d,  $J = 10.8$  Hz, 1 H), 3.79 (s, 3 H), 3.77–3.76 (m, 1 H), 3.58 (s, 1 H), 2.64 (s, 3 H), 2.20 (s, 3 H), 2.10 (d,  $J = 13.6$  Hz, 1 H), 1.77 (d,  $J = 12$  Hz, 2 H), 1.66 (d,  $J = 12.8$  Hz, 2 H), 1.49–1.42 (m, 2 H), 1.39–1.37 (m, 2 H), 1.28 (s, 9 H);  $^{13}\text{C}$  NMR ( $\text{CDCl}_3$ , 100 MHz): 160.3, 158.8, 158.6, 156.2, 152.3, 148.9, 148.9, 133.0, 129.2, 123.7, 122.3, 144.4, 114.1, 112.1, 111.7, 111.5, 76.6, 73.2, 69.2, 55.2, 43.1, 39.1, 35.4, 31.0, 29.2, 27.6, 24.9, 24.1, 19.9, 12.3; LCMS (ESI)  $[\text{M}+\text{H}]^+$ : 505.33. Anal. Calcd for  $\text{C}_{31}\text{H}_{37}\text{N}_2$ : C, 73.78; H, 7.39; N, 5.55. Found: C, 73.81; H, 7.35; N, 5.58.

### 2.1.4. 6-(*tert*-butyl)-1-((4-(4-chlorophenyl)-6,6-dimethyl-5,6-dihydro-4H-1,2-oxazin-3-yl)methyl)-8-fluoro-2,3-dimethylquinolin-4(1H)-one (3b)

433.2 mg (Yield 90 %); Off-white solid; mp:  $138\text{--}139^\circ\text{C}$ ; IR  $\sqrt{\text{max}}$ :  $1650\text{ cm}^{-1}$  ( $\nu_{\text{C=O}}$ ),  $1491.93\text{ cm}^{-1}$  ( $\nu_{\text{C-C}}$ ),  $1011.25\text{ cm}^{-1}$  ( $\nu_{\text{C-F}}$ ),

694.78  $\text{cm}^{-1}$   $\sqrt{(\text{C-Cl})}$ ;  $^1\text{H NMR}$  ( $\text{CDCl}_3$ , 400 MHz)  $\delta$ : 7.48 (s, 1 H), 7.38–7.34 (m, 3 H), (d, J = 8 Hz, 2 H), 4.53 (d, J = 12 Hz, 1 H), 4.29 (d, J = 8 Hz, 1 H), 3.82–3.78 (m, 1 H), 2.64 (s, 3 H), 2.17–2.12 (m, 1 H), 2.06 (s, 3 H), 1.92–1.86 (m, 1 H), 1.40–1.35 (m, 6 H), 1.32 (s, 9 H);  $^{13}\text{C NMR}$  ( $\text{CDCl}_3$ , 100 MHz): 160.3, 154.3, 149.1, 138.3, 133.4, 129.7, 129.4, 123.6, 122.2, 112.0, 111.7, 75.2, 73.5, 40.2, 37.0, 35.1, 31.0, 28.3, 24.0, 22.6, 12.2; LCMS (ESI)  $[\text{M}+\text{H}]^+$ : 483.27. Anal. Calcd for  $\text{C}_{28}\text{H}_{32}\text{N}_2$ : C, 69.62; H, 6.68; N, 5.80. Found: C, 69.67; H, 6.73; N, 5.79.

**2.1.5. 6-(tert-butyl)-1-((6,6-dimethyl-4-phenyl-5,6-dihydro-4H-1,2-oxazin-3-yl)methyl)-8-fluoro-2,3-dimethylquinolin-4(1H)-one (3c)**

394.2 mg (Yield 88 %); Off-white solid; mp: 140–141 °C; IR  $\sqrt{\text{max}}$ : 1601.47  $\text{cm}^{-1}$   $\sqrt{(\text{C=O})}$ , 1394.94  $\text{cm}^{-1}$   $\sqrt{(\text{C-C})}$ , 1060.9  $\text{cm}^{-1}$   $\sqrt{(\text{C-F})}$ , 1009.51  $\text{cm}^{-1}$   $\sqrt{(\text{C-O})}$ ;  $^1\text{H NMR}$  ( $\text{CDCl}_3$ , 400 MHz)  $\delta$ : 7.56 (s, 1 H), 7.35–7.31 (m, 5 H), 7.25–7.22 (m, 1 H), 4.53 (s, 1 H), 4.31 (d, J = 12 Hz, 1 H), 3.80 (s, 1 H), 2.63 (s, 3 H), 2.16 (s, 2 H), 8 (s, 3 H), 1.41–1.38 (m, 6 H), 1.33 (s, 9 H);  $^{13}\text{C NMR}$  ( $\text{CDCl}_3$ , 100 MHz): 160.3, 158.8, 154.9, 149.0, 139.8, 129.2, 128.3, 127.5, 123.7, 122.1, 112.2, 111.8, 111.6, 76.7, 75.2, 73.4, 40.4, 37.6, 35.1, 31.1, 28.3, 24.1, 22.7, 12.2; LCMS (ESI)  $[\text{M}+\text{H}]^+$ : 449.29. Anal. Calcd for  $\text{C}_{28}\text{H}_{33}\text{N}_2$ : C, 74.97; H, 7.42; N, 6.25. Found: C, 74.99; H, 7.45; N, 6.28.

**4-(4-chlorophenyl)-3-((4-((4-chlorophenyl)(phenyl)methyl)piperazin-1-yl)methyl)-6,6-dimethyl-5,6-dihydro-4H-1,2-oxazine (3d)**

428.6 mg (Yield 79 %); Off-white solid; mp: 132–133 °C;  $^1\text{H NMR}$  ( $\text{CDCl}_3$ , 400 MHz)  $\delta$ : 7.44–7.39 (m, 4H), 7.28–7.21 (m, 9H), 5.60 (s, 1 H), 4.17 (s, 2 H), 2.78–2.61 (m, 9H), 1.98–1.81 (m, 2H), 1.34 (s, 3 H), 1.23 (m, 3 H); LCMS (ESI)  $[\text{M}+\text{H}]^+$ : 523.52. Anal. Calcd for  $\text{C}_{30}\text{H}_{33}\text{Cl}_2\text{N}_3\text{O}$ : C, 68.96; H, 6.37; N, 8.04; Found: C, 68.98; H, 6.38; N, 8.06

**2.1.6. 4-((4-((4-chlorophenyl)(phenyl)methyl)piperazin-1-yl)methyl)-6,6-dimethyl-4-phenyl-5,6-dihydro-4H-1,2-oxazine (3e)**

281.6 mg (Yield 66 %); White solid; mp: 141–142 °C; IR  $\sqrt{\text{max}}$ : 2971.8  $\text{cm}^{-1}$   $\sqrt{(\text{C-H})}$ , 1489.64  $\text{cm}^{-1}$   $\sqrt{(\text{C-C})}$ , 1294.03  $\text{cm}^{-1}$   $\sqrt{(\text{C-C})}$ , 1092.92  $\text{cm}^{-1}$   $\sqrt{(\text{C-O})}$ , 720.15  $\text{cm}^{-1}$   $\sqrt{(\text{C-Cl})}$ ;  $^1\text{H NMR}$  ( $\text{CDCl}_3$ , 400 MHz)  $\delta$ : 7.33–7.27 (m, 7 H), 7.22–7.17 (m, 7 H), 4.17 (s, 1 H), 3.56 (t, J = 9 Hz, 1 H), 2.79 (d, J = 13.2 Hz, 1 H), 2.70 (d, J = 12.8 Hz, 1 H), 2.43–2.31 (m, 6 H), 2.10 (s, 2 H), 2.04–1.99 (m, 1 H), 1.94–1.88 (m, 1 H), 1.32 (s, 3 H), 1.20 (m, 3 H);  $^{13}\text{C NMR}$  ( $\text{CDCl}_3$ , 100 MHz): 157.0, 142.2, 141.3, 140.7, 132.5, 129.1, 128.6, 128.6, 127.7, 127.1, 126.9, 75.6, 74.3, 59.5, 53.0, 52.1, 39.9, 37.9, 28.5, 22.8; LCMS (ESI)  $[\text{M}+\text{H}]^+$ : 488.26. Anal. Calcd for  $\text{C}_{30}\text{H}_{34}\text{N}_3$ : C, 73.83; H, 7.02; N, 8.61. Found: C, 73.85; H, 7.04; N, 8.65.

**2.1.7. 3-((4-((4-chlorophenyl)(phenyl)methyl)piperazin-1-yl)methyl)-6,6-dimethyl-5,6-dihydro-4H-1,2-oxazine (3f)**

259.7 mg (Yield 70 %); Off-white solid; mp: 146–147 °C; IR  $\sqrt{\text{max}}$ : 1612.09  $\text{cm}^{-1}$   $\sqrt{(\text{C=O})}$ , 1512.04  $\text{cm}^{-1}$   $\sqrt{(\text{C-C})}$ , 1246.9  $\text{cm}^{-1}$   $\sqrt{(\text{C-C})}$ , 1034.19  $\text{cm}^{-1}$   $\sqrt{(\text{C-O})}$ , 725.76  $\text{cm}^{-1}$   $\sqrt{(\text{C-Cl})}$ ;  $^1\text{H NMR}$  ( $\text{CDCl}_3$ , 400 MHz)  $\delta$ : 7.99 (d, J = 6 Hz, 2 H), 7.58 (s, 1 H), 7.44–7.22 (m, 11 H), 5.64 (s, 1 H), 4.05 (s, 1 H), 3.39 (d, J = 12.8 Hz, 1 H), 3.08 (d, J = 12.8 Hz, 1 H), 2.45–2.33 (m, 4 H), 2.21 (s, 4 H), 1.97–1.95 (m, 1 H), 1.41–1.31 (m, 6 H);  $^{13}\text{C NMR}$ : 165.3, 153.0, 142.2, 141.3, 133.3, 132.4, 129.6, 129.1, 128.5, 127.7, 127.0, 75.4, 74.3, 60.3, 58.8, 53.2, 51.6, 36.4, 26.0, 25.4; LCMS (ESI)  $[\text{M}+\text{H}]^+$ : 532.26. Anal. Calcd for  $\text{C}_{31}\text{H}_{34}\text{ClN}_3\text{O}_3$ : C, 69.98; H, 6.44; N, 7.90; Found: C, 70; H, 6.46; N, 7.92.

**2.1.8. 3-((4-(1H-benzo[d]imidazol-2-yl)piperidin-1-yl)methyl)-4-(4-methoxyphenyl)-4a,5,6,7,8a-hexahydro-4H-benzo[e][1,2]oxazine (3g)**

524.1 mg (Yield 92 %); White solid; mp: 141–142 °C;  $^1\text{H NMR}$  ( $\text{CDCl}_3$ , 400 MHz)  $\delta$ : 7.51 (s, 2 H), 7.20–7.08 (m, 2 H), 6.98–6.90 (m, 2 H), 6.81–6.9 (m, 2 H), 4.17 (s, 2 H), 3.77 (s, 3 H), 3.58–3.51 (m, 1 H), 2.95–2.80 (m, 4 H), 2.17–2.01 (m, 1 H), 2.05–1.89 (m, 8 H), 1.39 (s, 3 H), 1.34 (s, 3 H);  $^{13}\text{C NMR}$  ( $\text{CDCl}_3$ , 100 MHz): 158.5, 157.7, 157.6, 132.5, 129.6, 122.1, 114.6, 74.3, 59.8, 55.2, 54.3, 51.8, 39.9, 37.0, 36.4, 31.3, 31.1, 28.5, 22.8; LCMS (ESI)  $[\text{M}+\text{H}]^+$ : 459.31. Anal. Calcd or  $\text{C}_{28}\text{H}_{34}\text{N}_4$ : C, 73.33; H, 7.47; N, 12.22. Found: C, 73.35; H, 7.49; N, 12.24.

**2.1.9. 3-((4-(1H-benzo[d]imidazol-2-yl)piperidin-1-yl)methyl)-4-(4-methoxyphenyl)-6,6-dimethyl-5,6-dihydro-4H-1,2-oxazine (3h)**

419.3 mg (Yield 78 %); Off-white solid; mp: 135–136 °C; IR  $\sqrt{\text{max}}$ : 1511.85  $\text{cm}^{-1}$   $\sqrt{(\text{NH})}$ , 1246.29  $\text{cm}^{-1}$   $\sqrt{(\text{C-C})}$ , 1032.8  $\text{cm}^{-1}$   $\sqrt{(\text{C-O})}$ ;  $^1\text{H NMR}$  ( $\text{CDCl}_3$ , 400 MHz)  $\delta$ : 9.3 (s, 1 H), 7.4–7.2 (m, 2 H), 7.1–7.0 (m, 2 H), 6.9–6.8 (m, 4 H) 5.0 (s, 2 H), 4.1–4.0 (m, 1 H), 3.8 (s, 3 H), 3.1–3.0 (m, 1 H), 2.8–2.7 (m, 2 H), 2.2–1.6 (m, 8 H), 1.4 (s, 3 H), 1.2 (s, 3 H); LCMS (ESI)  $[\text{M}+\text{H}]^+$ : 433.27. Anal. Calcd for  $\text{C}_{26}\text{H}_{32}\text{N}_4$ : C, 72.19; H, 7.46; N, 12.95. Found: C, 72.23; H, 7.42; N, 12.99.

**2.1.10. 3-((4-(1H-benzo[d]imidazol-2-yl)piperidin-1-yl)methyl)-4-phenyl-4a,5,6,7,7a-hexahydrocyclopenta[e][1,2]oxazine (3i)**

318.9 mg (Yield 77 %); Off-white solid; mp: 137–138 °C; IR  $\sqrt{\text{max}}$ : 2928.89  $\text{cm}^{-1}$   $\sqrt{(\text{C-H})}$ , 1610.38  $\text{cm}^{-1}$   $\sqrt{(\text{C=O})}$ , 1247.58  $\text{cm}^{-1}$   $\sqrt{(\text{C-C})}$ , 1034.22  $\text{cm}^{-1}$   $\sqrt{(\text{C-O})}$ ;  $^1\text{H NMR}$  ( $\text{CDCl}_3$ , 400 MHz)  $\delta$ : 7.59 (m, 2 H), 7.48 (m, 2 H), 7.29–7.13 (m, 5 H), 4.11 (s, 2 H), 3.41 (s, 1 H), 2.43 (m, 2 H), 2.17 (m, 2 H), 2.02–1.88 (m, 4 H), 1.71–1.41 (m, 10 H);  $^{13}\text{C NMR}$  ( $\text{CDCl}_3$ , 100 MHz): 164.6, 156.1, 156.8, 140.7, 139.2, 132.5,

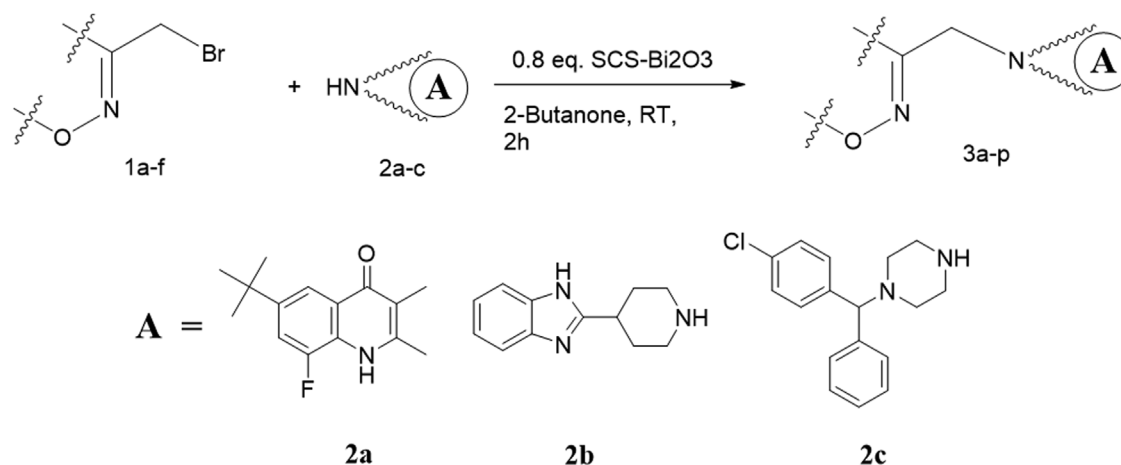


**Fig. 2.** The synthetic route for the preparation of title compounds (3a–j). 1a–f represents the bromides that are used in the preparation of 1,2-oxazines (3a–j) and structures of bromides are provided in Table 1.

130.0, 129.6, 121.5, 117.6, 74.02, 56.7, 54.4, 51.8, 40.3, 39.6, 37.1, 36.2, 31.2, 30.9, 28.4, 22.7; HRMS (ESI) (M + Na)<sup>+</sup>: 437.2316.

2.1.11. 3-((4-(1H-benzod[*j*]imidazol-2-yl)piperidin-1-yl)methyl)-6,6-dimethyl-5,6-dihydro-4H-1,2-oxazin-4-yl benzoate (3 j)

477.3 mg (Yield 86 %); Off-white solid; mp: 140–141 °C; IR  $\nu_{\text{max}}$ : 2934  $\text{cm}^{-1}$  ( $\nu_{\text{C-H}}$ ), 1610  $\text{cm}^{-1}$  ( $\nu_{\text{C=O}}$ ), 1510  $\text{cm}^{-1}$  ( $\nu_{\text{C=C}}$ ), 1247  $\text{cm}^{-1}$  ( $\nu_{\text{C-O}}$ ), 1034  $\text{cm}^{-1}$  ( $\nu_{\text{C-O}}$ ); <sup>1</sup>H NMR (CDCl<sub>3</sub>, 400 MHz)  $\delta$ : 7.55 (s, 2 H), 7.25–7.19 (m, 2 H), 7.05–7.03 (m, 2 H), 6.84–6.82 (m, 3 H), 4.01 (s, 1 H), 3.77 (s, 3 H), 3.44 (m, 1 H), 3.08–2.87 (m, 4 H), 2.74 d, J = 10 Hz, 2 H), 2.22–2.01 (m, 8 H), 1.35 (s, 3 H), 1.24 (s, 3 H); <sup>13</sup>C NMR (CDCl<sub>3</sub>, 100 MHz): 158.4, 157.6, 154.2, 133.7, 129.3, 122.2, 114.3, 114.1, 60.1, 55.2, 54.4, 51.9, 42.9, 38.7, 36.2, 30.9, 30.7, 29.2, 27.5, 25.0, 19.9; LCMS (ESI) [M+H]<sup>+</sup>: 447.24. Anal. Calcd for C<sub>26</sub>H<sub>30</sub>N<sub>4</sub>: C, 69.93; H, 6.77; N, 12.55. Found: C, 69.95; H, 6.79; N, 12.58.

## 2.2. Pharmacology

### 2.2.1. MTT assay

Cytotoxicity of the newly synthesized compounds was evaluated using MTT assay against hepatocellular carcinoma cells as described previously [51]. Briefly, HepG2 and HCCLM3 liver cancer cells were cultured in DMEM containing 10 % FBS. For cytotoxicity assay (5 × 10<sup>3</sup>/well) were incubated in triplicate in a 96-well plate, in the presence of different concentrations of compounds at a volume of 0.2 mL, for different time intervals at 37 °C. Thereafter, 20  $\mu\text{L}$  MTT solution (5 mg/mL in PBS) was added to each well. After 2 h of incubation at 37 °C, the media was carefully removed, and the purple crystals were dissolved in 0.1 mL of DMSO. Finally, the optical density (OD) at 570 nm was measured using the Tecan plate reader.

### 2.2.2. Flow cytometric analysis

Flow cytometric analysis was performed to determine whether **3i** can induce apoptosis of HepG2 and HCCLM3 cells. Briefly, hepatocellular carcinoma cells (5 × 10<sup>5</sup>) were plated in a 60 mm petri dish and 24 h later the cells were exposed to compound **3i** (50  $\mu\text{M}$ ) for 0, 24, 48 and 72 h. Thereafter cells were washed, fixed with 70 % ethanol, and incubated for 30 min at 37 °C with 0.1 % RNase A in PBS. Cells were washed again, resuspended, and stained with PBS containing 25  $\mu\text{g}/\text{mL}$  propidium iodide (PI) for 15 min at room temperature. The cell cycle distribution across the various phases was analyzed using the flow cytometer.

### 2.2.3. Annexin V/PI apoptosis assay

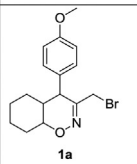
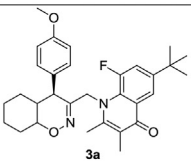
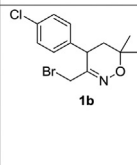
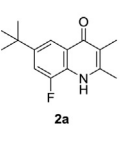
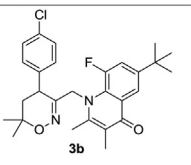
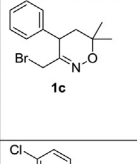
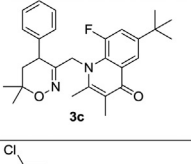
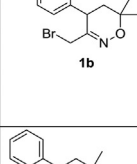
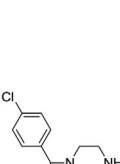
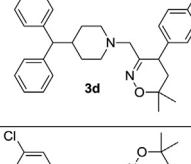
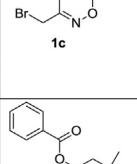
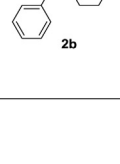
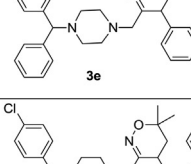
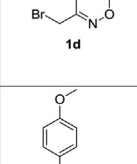
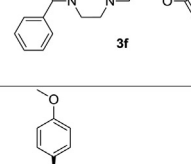
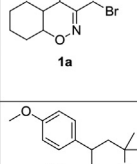
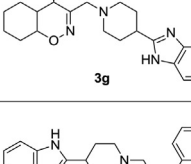
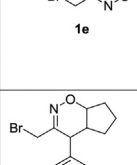
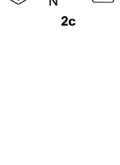
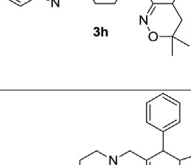
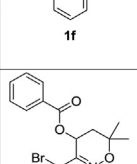
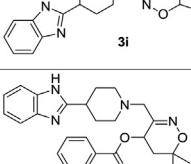
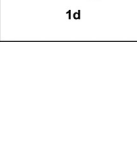
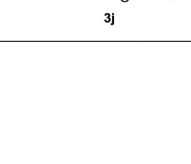
Phosphatidylserine exposure and cell death were assessed by FACS analysis using Annexin-V-PI-stained cells as described previously [57,58]. Briefly, 5 × 10<sup>5</sup> HepG2 cells were seeded in a 60 mm petri dish and incubated with **3i** (50  $\mu\text{M}$ ) for indicated time points and DMSO treated samples were used as a control. Cells were then washed with Annexin V binding buffer (10 mM HEPES/NaOH, pH7.4, 140 mM NaCl, 2.5 mM CaCl<sub>2</sub>), stained with Annexin V FITC for 30 min at room temperature in the dark, then washed again and resuspended in Annexin V binding buffer containing PI. Samples were analyzed immediately using the flow cytometer.

### 2.2.4. DNA fragmentation assay

DNA fragmentation assay was performed using the Cell Death Detection ELISA<sub>PLUS</sub> assay kit (Roche, CA, USA) according to the manufacturer's instructions. Briefly, HepG2 cells were plated in 6-well plates and allowed to adhere for 24 h. HepG2 cells were then transfected with either control siRNA or

**Table 1**

The physical parameters of the newly synthesized oxazine derivatives.

Bromide (1a-f)	Amine (2a-e)	Product (3a-n)	Yield (%)	HepG2 IC <sub>50</sub> ( $\mu\text{M}$ )
			78	>50
			90	>50
			88	>50
			79	NT
			66	NT
			70	NT
			92	>50
			78	>50
			77	46.4
			86	>50

NF- $\kappa$ B-siRNA for 48 h and then treated with compound **3i** 25 or 50  $\mu$ M for an additional 72 h after which the media was aspirated, the cells were washed with cold PBS and incubated on ice for 30 min in cell lysis buffer. The cells were then scraped and the lysates were collected in a centrifuge tube and vortexed to break up the cell aggregates. The lysates were cleared by centrifugation at 5000 rpm for 10 min at 4 °C and the supernatant were stored at -80 °C. The cell lysates were added to lysis buffer provided with the kit and pipetted on streptavidin coated 96-well microtiter plate to which immunoreagent mix was added and incubated for 2 h at room temperature with continuous shaking at 500 rpm. The wells were then washed with washing buffer, and the color was developed by the addition of a substrate solution, which was read at 405 nm against the blank, reference wavelength of 490 nm after 10–15 min. The enrichment factor (total amount of apoptosis) was calculated by dividing the absorbance of the sample (A405 nm) by the absorbance of the controls without treatment (A490 nm).

### 2.2.5. Western blot assay

HepG2 and MDA-MB-231 cells were plated in 6-well plates and allowed to adhere for 24 h. On the day of transfection, lipofectamine was added to control or NF- $\kappa$ B siRNA (100 nM) in a final volume of 1 mL of culture medium. After 48 h of incubation following transfection, the cells were lysed and 50  $\mu$ g protein was taken for Western blot analysis. Briefly, 50  $\mu$ g of nuclear proteins extracted from treated or control cells were resolved in 10 % SDS gel. After electrophoresis, the proteins were electro-transferred to a nitrocellulose membrane (Bio-Rad, USA), blocked with Blocking One (Nacalai Tesque, Inc, Japan), and probed with p65 and  $\beta$ -actin primary antibody overnight at 4 °C. The blot was washed and probed with horseradish peroxidase-conjugated secondary antibody for 1 h and finally examined by chemiluminescence substrate (ECL, GE Healthcare, UK).

### 2.2.6. NF- $\kappa$ B DNA binding assay

Activation of NF- $\kappa$ B was evaluated by DNA binding assay using TransAM NF- $\kappa$ B Kit according to the manufacturer's instructions. Briefly, 50  $\mu$ g of nuclear protein was extracted from 0, 10, 25 and 50  $\mu$ M **3i** treated cells for 8 h and were added into 96-well plate coated with an unlabelled oligonucleotide containing the discrete single-stranded consensus binding site for NF- $\kappa$ B (5'-GGGACTTTC-3') and incubated for 1 h. The wells were washed and incubated with antibodies against NF- $\kappa$ B p65 subunit. An HRP conjugated secondary antibody was then applied to detect the bound primary antibody. HRP substrate was added and the color produced provided the basis for colorimetric quantification as per kit manufacturer instructions.

### 2.2.7. NF- $\kappa$ B luciferase reporter assay

The effect of **3i** on constitutive NF- $\kappa$ B-dependent reporter gene transcription in HepG2 and HCCLM3 cells was determined. NF- $\kappa$ B responsive elements linked to a luciferase reporter gene were transfected with wild-type or dominant-negative I $\kappa$ B. The transfected cells were then treated with various doses of **3i** for 6 h. Luciferase activity was measured with a Tecan (Durham, NC, USA) plate reader and normalized to  $\beta$ -galactosidase activity. All luciferase experiments were done in triplicate and repeated twice.

### 2.2.8. In silico interaction analysis

Discovery Studio 2.5 software from Accelrys was used for docking and visualization of the results. Initially, we retrieved the crystal structure of the NF- $\kappa$ B p65 homodimer complex with a DNA (PDB ID: 1RAM, 2.4 Å resolution) cleaned, minimized the energy, and identified the spatial region of p65. All the energy calculations were performed using the CHARMM force field. The three-dimensional structures of all 1,2-oxazines were prepared and docked toward the p65 using the LigandFit protocol of Discovery Studio. The binding pose of ligands was evaluated using the interaction score function in the Ligand Fit module of Discovery Studio.

## 3. Results

### 3.1. Chemistry

#### 3.1.1. Preparation of 1,2 oxazines

The substituted bromomethyl 1,2-oxazine derivatives were prepared as described earlier [49]. Given the biological significance of oxazines in NF- $\kappa$ B inhibition, we synthesized the new derivatives of (**1**) via a C–N bond formation reaction as presented in Fig. 2. In the present synthetic strategy, we utilized three different secondary amines namely, 6-(tert-butyl)-8-fluoro-2,3-dimethylquinolin-4(1H)-one (**2a**), 1-((4-chlorophenyl)(phenyl)methyl)piperazine (**2b**), and 2-(piperidin-4-yl)-1H-benzo[d]imidazole (**2c**) for the preparation of title compounds. Based on our previous experience, the utilization of these secondary amine intermediates (**2a-c**) resulted in products with good biological activity and therefore **2a-c** were chosen for coupling reactions in the present study. Based on our earlier report [38,50], we utilized the mild basic characteristic of combustion-derived Bi<sub>2</sub>O<sub>3</sub> (SCS-Bi<sub>2</sub>O<sub>3</sub>) to prevent the decomposition of base sensitive bromomethyl 1,2-oxazine (**1**) and for C–N bond formation reaction. The synthesis of the final product (**3a-j**) was achieved in good yield. All the newly synthesized oxazine derivatives were characterized by <sup>1</sup>H NMR, <sup>13</sup>C NMR, CHN, and mass analysis and structures are

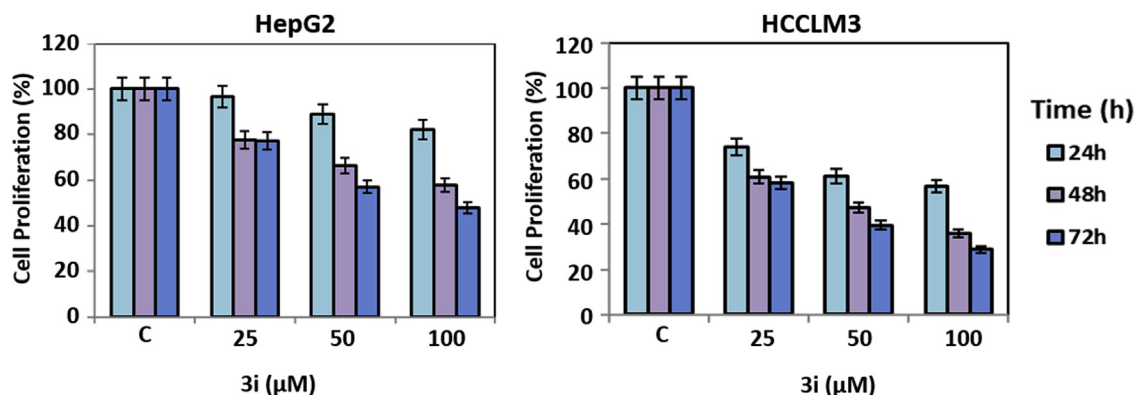
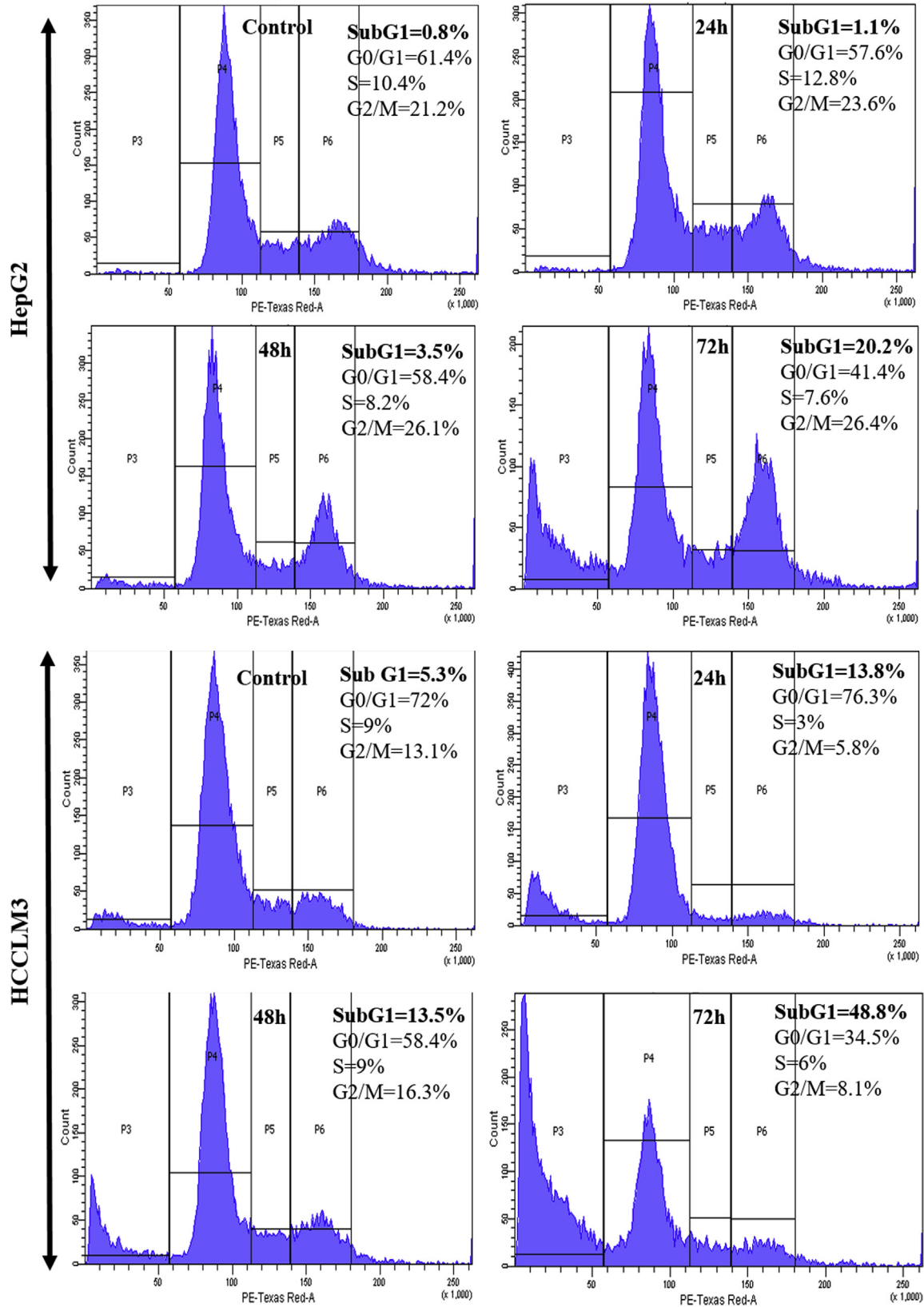
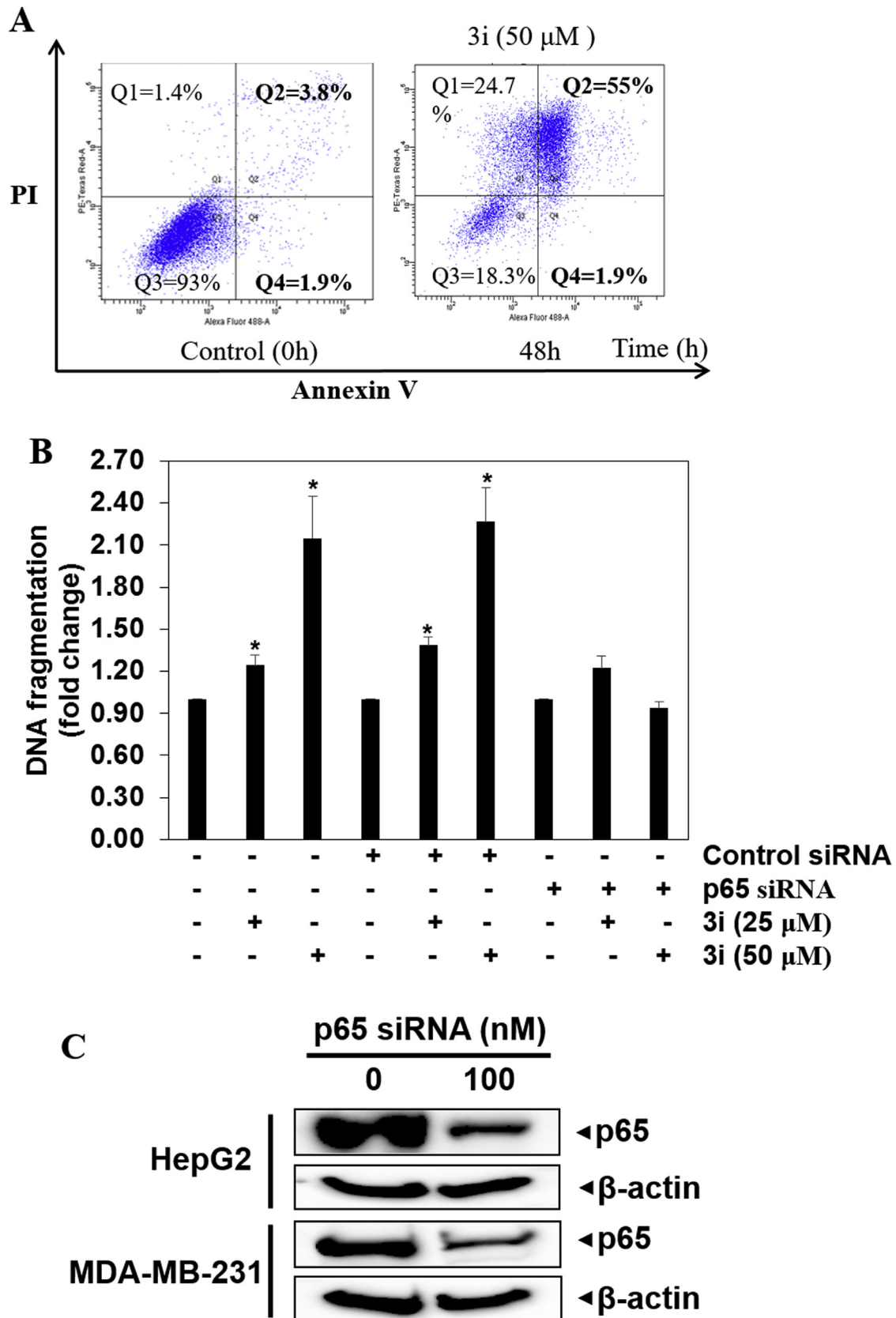


Fig. 3. **3i** elicits growth inhibitory effects in HCC cells. HepG2 and HCCLM3 cells were treated with different concentrations (25, 50 and 100  $\mu$ M) of **3i** at indicated time intervals (24, 48, and 72 h) and then subjected to MTT assay as described in materials and methods (\* $p$  < 0.05).

Figure 4



**Fig. 4.** 3i induced apoptosis in HCC cells. The distribution of cell cycle in 3i treated HepG2 and HCLM3 cells were examined using flow cytometry. Cells were exposed to 3i (50  $\mu$ M) at indicated times (0, 24, 48 and 72 h), after which cells were harvested and stained with propidium iodide.



**Fig. 5.** (A) 3i induced apoptosis in HepG2 cells. Cells were exposed to 3i (50  $\mu$ M) for 48 h, after which cells were harvested and stained with Annexin V and propidium iodide. The percentage of early and late apoptotic cells were detected using flow cytometry. Results show early apoptosis, defined as annexin V-positive and PI-negative cells, and late apoptosis, defined as annexin V-positive and PI-positive cells. (B) The knockdown of p65 by small interfering RNA (siRNA) reduces the 3i-induced DNA fragmentation. HepG2 cells were transfected with either control or p65 specific siRNA (50 nM). After 48 h, the cells were treated with 3i (25 or 50  $\mu$ M) for 72 h, and the DNA fragmentation was analyzed by the ELISA assay kit. The data is expressed as mean  $\pm$  SD, compared with the untreated control, (\* $p$  < 0.05). (C) Western blot analysis revealed that siRNA efficiently knocked down NF- $\kappa$ B-p65 in both the cell lines tested.

shown in Table 1 and spectra are provided as supporting information.

### 3.2. Pharmacology

#### 3.2.1. 1,2-Oxazines elicit growth inhibitory effect in HCC cells

Previous studies suggested that oxazine derived compounds possess good anticancer activity towards various cancer models. Initially, we tested the anticancer potential of all the newly synthesized compounds against HepG2 cells using MTT assay [51,52]. Among the tested compounds, **3e** and **3i** were found to be good anticancer agents with  $IC_{50}$  values of 47.6 and 46.4  $\mu$ M. The  $IC_{50}$  values were determined using GraphPad Prism software [15]. The  $IC_{50}$  value of other compounds towards HepG2 cells is provided in Table 1. Since compound **3i** showed relatively better anticancer potential, we further investigated the effect of **3i** on the proliferation of HCCLM3 cells. Compound **3i** exhibited good anticancer potential towards HCCLM3 with an  $IC_{50}$  value of 40.9  $\mu$ M. Furthermore, we treated HepG2 and HCCLM3 cells with **3i** in different time-points at different doses as indicated in Fig. 3. Compound **3i** significantly reduced the proliferation of both the cell lines in a dose- and time-dependent manner (Fig. 3). We next evaluated the effect of **3i** against normal hepatocytes (LO2) and did not find significant cytotoxicity of the compound towards normal cells (Data not shown). Doxorubicin and paclitaxel are used as reference compounds and  $IC_{50}$  values are 10 and 8 nM, respectively towards HCCLM3 cells. The results indicate that the presence of cyclopentane ring fused to the 1,2-oxazine heterocycle enhances the cytotoxic effect towards HCC cells.

#### 3.2.2. **3i** increases the subG1 population in HCC cells

The activation of executioner caspases and caspase-activated DNases during apoptosis leads to the cleavage of genomic DNA into oligonucleotide fragments and the cells with reduced DNA are detected as subG1 cell population [53,54]. Therefore, we treated HepG2 and HCCLM3 cells with **3i** for different time intervals and analyzed the distribution of cells in various phases of the cell cycle using propidium iodide staining as described earlier [55,56]. The results indicated that **3i** caused a substantial increase in the accumulation of the subG1 population to 20.2 % in HepG2 and 48.8 % in HCCLM3 cells in a time-dependent manner (Fig. 4). The results clearly demonstrated the apoptosis inducing effect of **3i** in HCC cells.

#### 3.2.3. **3i** induces apoptosis in HCC cells

The appearance of phosphatidylserine in the outer leaflet of the plasma membrane is one of the biochemical events in the cell committed to apoptosis which can be detected using annexin V-FITC-PI staining [57,58]. We next examined the effect of **3i** on the translocation of phosphatidylserine in HepG2 cells. **3i** significantly increased the percentage of apoptotic cells (55 %) compared with DMSO-treated cells (3.8 %) (Fig. 5A). These findings provide another direct evidence for apoptosis inducing effect of **3i**.

#### 3.2.4. Transfection with p65 siRNA blocks **3i** induced DNA fragmentation in HCC cells

DNA fragmentation is one of the key events in the cells undergoing apoptosis [59,60]. Hence, we investigated whether the knockdown of NF- $\kappa$ B using siRNA could inhibit the **3i** induced DNA

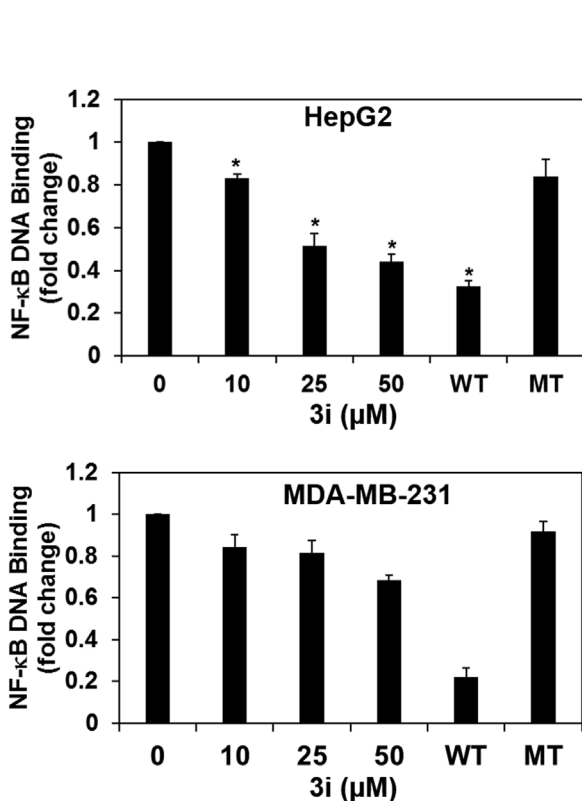


**Fig. 6.** (A) The effect of **3i** on the constitutive DNA-binding activity of NF- $\kappa$ B. **3i** downregulated NF- $\kappa$ B DNA binding ability in HepG2 and MDA-MB-231 cells. The cells were treated with 0, 10, 25 and 50  $\mu$ M **3i** for 8 h and nuclear extracts were prepared and 50  $\mu$ g of nuclear extract protein was used for DNA binding assay. The NF- $\kappa$ B DNA binding was inhibited in a dose-dependent manner. WT (wild type oligonucleotide); MT (mutant oligonucleotide). **3i** was found to reduce the DNA-binding activity of constitutively activated NF- $\kappa$ B.

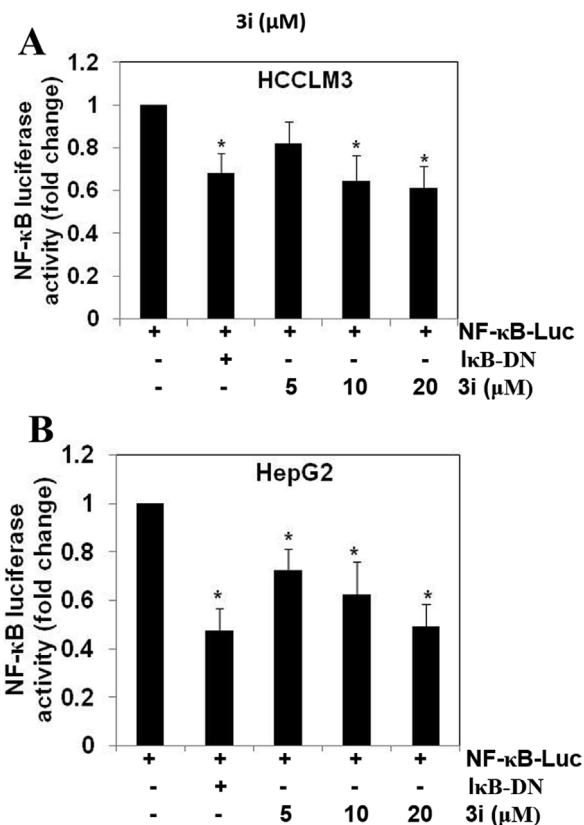


**Fig. 7.** (A and B) **3i** suppresses constitutive activation of reporter gene expression. HepG2 ( $5 \times 10^5$ /mL) and HCCLM3 ( $5 \times 10^5$ /mL) cells were transfected with NF- $\kappa$ B luciferase and  $\beta$ -galactosidase reporter plasmid using lipofectamine, incubated for 24 h, and then treated with **3i** for 5, 10, and 20 h. Cells were lysed in reporter lysis buffer and analyzed for luciferase activity and normalized with  $\beta$ -galactosidase activity. Results are expressed as fold activity over the activity of vector control. \* $p < 0.05$ .



fragmentation in HepG2 cells. In **3i**-treated, control siRNA transfected cells, we observed a significant increase in DNA fragmentation (Fig. 5B). In the cells transfected with NF- $\kappa$ B siRNA, we observed the significant decline in the **3i** induced DNA fragmentation compared to control siRNA treated group indicating that, **3i** mediate its proapoptotic effects by abrogating NF- $\kappa$ B signaling pathway in HepG2 cells. The efficiency of transfection was further confirmed using western blotting analysis. The treatment of HepG2 and MDA-MB-231 cells with siRNA efficiently down-regulated the protein levels of NF- $\kappa$ B-p65 (Fig. 5C).

### 3.2.5. **3i** inhibits the constitutive activation of NF- $\kappa$ B in HCC cells

Oh et al., identified 7-benzoyl-4-phenylcyclopenta [1,2]oxazine as a potent IKK $\beta$  inhibitor out of 7243 diverse compounds which leads to the abrogation of NF- $\kappa$ B signaling pathway [61]. Hence, we evaluated whether **3i** could inhibit the constitutive activation of NF- $\kappa$ B in HepG2 and MDA-MB-231 cells. Initially, cancer cells were treated with 10, 25 and 50  $\mu$ M of **3i** followed by preparation of nuclear extract and evaluation for NF- $\kappa$ B DNA activity. We observed a significant decrease in DNA binding ability of NF- $\kappa$ B on **3i** treatment in a dose dependent fashion, thus indicating that **3i** can also attenuate NF- $\kappa$ B activation in different tumor cell lines (Fig. 6). The binding characteristics were typical for NF- $\kappa$ B transcription factors as noted by competition experiments with NF- $\kappa$ B-binding wild type (WT) DNA oligonucleotides or mutated (MT) oligonucleotides in DNA binding assay (Fig. 6). We next examined the effect of **3i** on the constitutive expression of the NF- $\kappa$ B-dependent reporter gene in HCC cells. HCC cells were transfected with NF- $\kappa$ B responsive elements linked with luciferase reporter gene with wild-type or dominant-negative I $\kappa$ B to study the effect of **3i** on constitutive activation of NF- $\kappa$ B. We observed a gradual decline in the expression of NF- $\kappa$ B-dependent reporter gene in the presence of **3i** with the maximum inhibition observed at 20  $\mu$ M (Fig. 7A and B). These results indicate that **3i** can potently affect the constitutive activation of the NF- $\kappa$ B signaling pathway.

### 3.2.6. *In silico* interaction analysis of oxazines with p65

1,2-oxazines are reported as good anticancer agents and they induce anticancer activity via inhibition of NF- $\kappa$ B at least partly in various cancer models. The oxygen-containing heterocyclic compounds such as helenalin selectively alkylate the p65 subunit and

inhibit the activation of NF- $\kappa$ B [62]. Here we used the crystal structure of homodimer of p65 with DNA for *in silico* interaction analysis targeting the key amino acids of p65 that interacts with DNA using the Discovery Studio LigandFit protocol [63]. Initially, we retrieved the crystal structure of the NF- $\kappa$ B p65 homodimer complex with a DNA (PDB ID: 1RAM, 2.4 Å resolution) cleaned, minimized the energy, and identified the spatial region of p65. All the energy calculations were performed using the CHARMM force field. The three-dimensional structures of all 1,2-oxazines were prepared and docked toward the p65 using the LigandFit protocol of Discovery Studio. The binding pose of ligands was evaluated using the interaction score function in the LigandFit module of Discovery Studio. The docking results were summarised in Table 2. The molecular interaction analysis revealed that the oxazines showed favorable interaction with the target protein with docking scores (DS) ranging from 48 to 62 kcal/mole. Interestingly, compound **3i** showed the DS of 54 kcal/mole indicating that it has a relatively high affinity towards p65. Additionally, the **3i** established hydrophobic interaction with Tyr36 and Arg187 of p65, which are present at the vicinity of the hydrophobic region near Cys38 of p65 protein (Fig. 8A-C). In addition, we compared the binding affinity of compound **3i** with a previously reported NF- $\kappa$ B inhibitor named CPP from our laboratory [21]. CPP presented the docking score of 56 kcal/mole which is comparable to compound **3i** and the interaction map of CPP with p65. These results indicate that the compound **3i** has a relatively better affinity for p65.

## 4. Discussion

Oxazine is a six-membered heterocycle with oxygen and nitrogen as a heteroatom and this ring system has been the part of various biologically active compounds. Oxazine derivatives were demonstrated to exhibit good cytotoxic potential in different types of cancer cell lines and *in vivo* models. In our previous study, an oxazine named CIMO inhibited the STAT3 signaling in HCC cell lines and the orthotopic nude mice model [36]. Srinivas and colleagues showed that 1,2-oxazines inhibit COX2 with high selectivity over COX1 [38]. In another study, pyridine conjugated oxazinones abrogated NF- $\kappa$ B signaling and induced apoptosis of HCC cells [14]. We also have shown that 1,2-oxazines inhibit the

**Table 2**

*In silico* interaction results of p65 with oxazines.

Entry	Mol. Weight	LS1D	LS2D	PLP1	PLP2	JAIN	-PMF	-LE	DS
3a	467.35	2.88	4.15	52.71	54.33	-2.41	56.66	-18.45	61.34
3b	450.77	2.52	4.29	34.6	41.84	-2.05	10.08	-9.31	52.67
3c	415.32	2.27	4.21	38.02	37.13	-1.92	64.01	-13.79	53.95
3d	407.75	2.04	4.33	49.9	50.51	-0.79	39.59	-5.04	50.70
3e	453.8	2.05	4.45	60.69	60.82	-0.58	34.26	-8.24	58.15
3f	497.81	3.46	4.99	57.4	60.41	-0.99	33.45	-11.49	57.82
3g	424.33	4.04	3.79	36.38	34.15	-0.92	57.24	-11.83	53.83
3h	400.31	4.03	4.24	44.66	39.87	-1.01	49.35	-10.5	56.16
3i	384.31	1.74	3.87	51.15	48.75	-0.91	36.15	-10.48	53.87
3j	416.31	2.27	4.53	55.77	53.53	-1.38	60.66	-9.50	56.27
CPP	366.07	2.23	4.35	63.21	59.60	-0.75	32.31	-7.24	56.12

LS1 and LS2: LigScore1 and 2 are a fast, simple, scoring function for predicting protein-ligand binding affinities.

PLP1 and PLP2, piecewise linear potentials 1 and 2 are fast, simple, docking function, that has been shown to correlate well with protein-ligand binding affinities.

JAIN, an empirical scoring function (lipophilic, polar attractive, and polar repulsive, interactions, solvation of the protein and ligand, and an entropy term for the ligand), through an evaluation of the structures and binding affinities of a series of protein-ligand complexes.

PMF, potential of mean force is the scoring function developed based on statistical analysis of the 3D structures of protein-ligand complexes.

DS, Dock Score, ligand poses are evaluated and prioritized according to the Dock Score function.

CPP is the previously reported NF- $\kappa$ B inhibitor and it has been used as the reference compound.

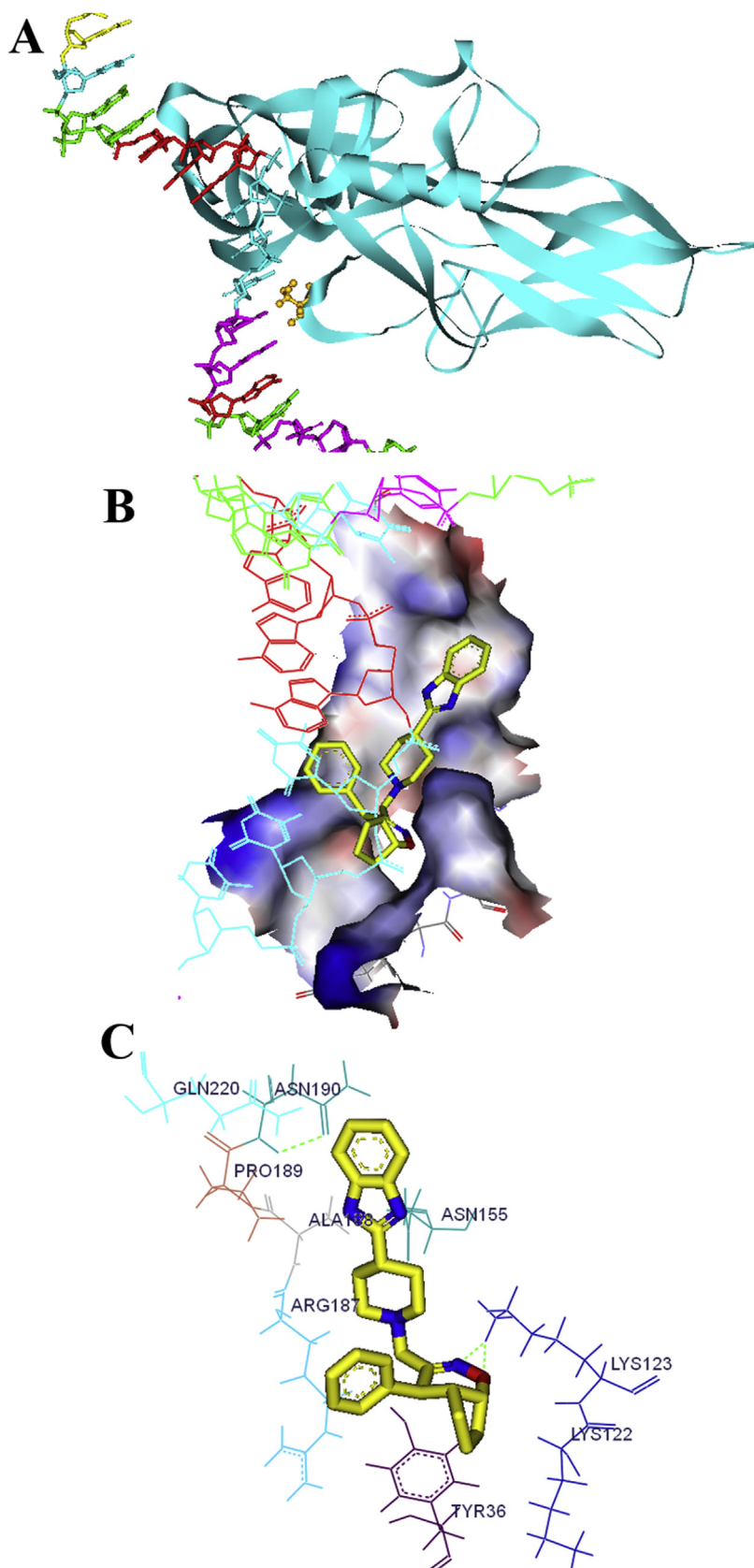


**Fig. 8.** *In silico* molecular interactions between p65 of NF- $\kappa$ B complex and the oxazines: (A) DNA bound p65 subunit is shown, where the stick form of the amino acid Cys38 region was used for docking studies (B & C) The surface view and interaction map for the lead compound **31** interaction with p65 subunit in the hydrophobic region is shown. **31** established hydrophobic interaction with Tyr 36 and Arg 187 of p65, which are present at the vicinity of the hydrophobic region near Cys38 of p65 protein.

growth of colon cancer cells by targeting the NF- $\kappa$ B signaling pathway and good anti-inflammatory activity was pronounced in inflammatory bowel disease mice model [37]. Therefore, in continuation of our attempts to explore oxazine derived potent NF- $\kappa$ B inhibitors, we prepared new 1,2-oxazine derivatives and evaluated for cytotoxic potential towards HCC cells. We used HCC cells which possess constitutive activation of NF- $\kappa$ B such as HepG2 and HCCLM3. Among the new chemical reagents, 3i showed relatively good cytotoxicity than other structural analogs without significantly affecting the viability of normal cells. Mansouri and colleagues also reported the similar cytotoxicity profile of oxazine derivatives towards chronic lymphocytic leukemia, colon and breast cancer cells and less toxic effects towards non-cancerous peripheral blood mononuclear cells [64]. However, the cytotoxic effect of the lead compound (3i) was significantly less compared to the standard therapeutic agents such as doxorubicin and paclitaxel.

The genomic DNA is fragmented during apoptosis and these cells are recognized as subG1 population in flow cytometric analysis [65]. 3i presented the increase in subG1 cells indicating its proapoptotic activity and this effect was further confirmed by annexin V-FITC-PI staining. 3i significantly increased the FITC-PI stained cells indicating phosphatidylserine externalization and internalization of propidium iodide. Furthermore, a large number of human cancers possess persistent activation of NF- $\kappa$ B due to oncogenic mutations and proinflammatory microenvironment and NF- $\kappa$ B has been entangled with the initiation and progression of cancer and metastasis [66–68]. We have previously demonstrated that NF- $\kappa$ B modulators induce apoptosis in cancer cells [69–71]. Treatment of NF- $\kappa$ B-p65 siRNA transfected cells with 3i did not show increased DNA fragmentation, whereas the treatment of scrambled siRNA transfected cells with 3i showed elevated DNA fragmentation. These results indicated that 3i mediates proapoptotic effect only *via* targeting NF- $\kappa$ B signaling and knockdown of p65 nullified the proapoptotic effect of 3i. By this result, we predict that 3i may not be an effective cytotoxic agent towards NF- $\kappa$ B-negative cancer cells. Persistent activation of NF- $\kappa$ B is seen in a wide range of tumors and its overexpression can be a predictive marker of negative prognosis [72–74]. Although all the assays were performed with HCC cell lines, we were interested to understand the effect of 3i on breast cancer cell line which possesses constitutively active NF- $\kappa$ B. Therefore, we selected two NF- $\kappa$ B expressing cancer cell lines (HepG2 and MDA-MB-231) of different tissue origin (liver and breast respectively) and tested the effect of 3i on the DNA binding ability of NF- $\kappa$ B. Compound 3i decreased the DNA binding ability of NF- $\kappa$ B in both cell lines suggesting that 3i interferes with the transcriptional activity of NF- $\kappa$ B. The transcription inhibitory effect of 3i was pronounced by the results of luciferase reporter gene expression. In conclusion, we report a new oxazine derived NF- $\kappa$ B inhibitor in HCC cells and validated in cell-based experiments and *in silico* analysis. Although the present investigation establishes NF- $\kappa$ B as the major cellular target of oxazines, the further detailed study is essential to learn about its off-targets, toxicity, and *in vivo* effects in suitable tumor models.

#### Author contributions

CS, SA, D, CPB, SM, and MKS performed the experiments. SR, AC, TAA, SAA, AS, CDM, B and KSR provided the resources. CDM, B, and KSR wrote the manuscript.

#### Declaration of Competing Interest

None declared.

#### Acknowledgments

This research was supported by the Department of Biotechnology-NER (BT/PR24978/NER/95/938/2017), Council of Scientific and Industrial Research (No. 02(0291)17/EMR-II), Vision group on Science and Technology, Government Of Karnataka (CESEM/GRD637-2018) to Basappa. This project was also supported by Researchers Supporting Project number (RSP-2019/5) King Saud University, Riyadh, Saudi Arabia. Authors thank Institution of Excellence (IOE) and Department of Science & Technology-Promotion of University Research and Scientific Excellence (DST-PURSE), University of Mysore for providing laboratory facility and financial assistance.

#### Appendix A. Supplementary data

Supplementary material related to this article can be found, in the online version, at doi:<https://doi.org/10.1016/j.btre.2020.e00438>.

#### References

- [1] S. Shishodia, B.B. Aggarwal, Nuclear factor-kappaB: a friend or a foe in cancer? *Biochem. Pharmacol.* 68 (2004) 1071–1080.
- [2] Y.R. Puar, M.K. Shanmugam, L. Fan, F. Arfuso, G. Sethi, V. Tergaonkar, Evidence for the involvement of the master transcription factor NF-kappaB in Cancer initiation and progression, *Biomedicines*. 6 (2018).
- [3] R. Ningegowda, N.S. Shivananju, P. Rajendran, K.S. Basappa, A. Rangappa, F. Chinnathambi, R.R. Li, M.K. Achar, P. Shanmugam, S.A. Bist, L.H.K. Alharbi, G. Lim, B.S. Sethi, Priya, A novel 4,6-disubstituted-1,2,4-triazolo-1,3,4-thiadiazole derivative inhibits tumor cell invasion and potentiates the apoptotic effect of TNFalpha by abrogating NF-kappaB activation cascade, *Apoptosis*. 22 (2017) 145–157.
- [4] F. Li, J. Zhang, F. Arfuso, A. Chinnathambi, M.E. Zayed, S.A. Alharbi, A.P. Kumar, K.S. Ahn, G. Sethi, NF-kappaB in cancer therapy, *Arch. Toxicol.* 89 (2015) 711–731.
- [5] S.C. Gupta, C. Sundaram, S. Reuter, B.B. Aggarwal, Inhibiting NF-kappaB activation by small molecules as a therapeutic strategy, *Biochim. Biophys. Acta* 1799 (2010) 775–787.
- [6] C. Kim, S.K. Cho, K.D. Kim, D. Nam, W.S. Chung, H.J. Jang, S.G. Lee, B.S. Shim, G. Sethi, K.S. Ahn, Beta-Caryophyllene oxide potentiates TNFalpha-induced apoptosis and inhibits invasion through down-modulation of NF-kappaB-regulated gene products, *Apoptosis*. 19 (2014) 708–718.
- [7] F. Li, M.K. Shanmugam, L. Chen, S. Chatterjee, J. Basha, A.P. Kumar, T.K. Kundu, G. Sethi, Garcinol, a polyisoprenylated benzophenone modulates multiple proinflammatory signaling cascades leading to the suppression of growth and survival of head and neck carcinoma, *Cancer Prev. Res. Phila. (Phila)* 6 (2013) 843–854.
- [8] G. Sethi, V. Tergaonkar, Potential pharmacological control of the NF-kappaB pathway, *Trends Pharmacol. Sci.* 30 (2009) 313–321.
- [9] R. Sen, D. Baltimore, Multiple nuclear factors interact with the immunoglobulin enhancer sequences, *Cell*. 46 (1986) 705–716.
- [10] G. Sethi, M.K. Shanmugam, L. Ramachandran, A.P. Kumar, V. Tergaonkar, Multifaceted link between cancer and inflammation, *Biosci. Rep.* 32 (2012) 1–15.
- [11] K.S. Siveen, N. Mustafa, F. Li, R. Kannaiyan, K.S. Ahn, A.P. Kumar, W.J. Chng, G. Sethi, Thymoquinone overcomes chemoresistance and enhances the anticancer effects of bortezomib through abrogation of NF-kappaB regulated gene products in multiple myeloma xenograft mouse model, *Oncotarget*. 5 (2014) 634–648.
- [12] A.S. Nair, S. Shishodia, K.S. Ahn, A.B. Kunnumakkara, G. Sethi, B.B. Aggarwal, Deguelin, an Akt inhibitor, suppresses IkkappaBalpha kinase activation leading to suppression of NF-kappaB-regulated gene expression, potentiation of apoptosis, and inhibition of cellular invasion, *J. Immunol.* 177 (2006) 5612–5622.
- [13] C.D. Mohan, N.C. Anilkumar, S. Rangappa, M.K. Shanmugam, S. Mishra, A. Chinnathambi, S.A. Alharbi, A. Bhattacharjee, G. Sethi, A.P. Kumar, K. Basappa, S. Rangappa, Novel 1,3,4-Oxadiazole induces anticancer activity by targeting NF-kappaB in hepatocellular carcinoma cells, *Front. Oncol.* 8 (2018) 42.
- [14] C.D. Mohan, H. Bharathkumar, S. Dukanya, M.K. Rangappa, A. Shanmugam, S.A. Chinnathambi, T.A. Alharbi, A. Alahmadi, P.E. Bhattacharjee, A. Lobie, K.M. Deivasigamani, G. Hui, Basappa Sethi, K.S. Rangappa, A.P. Kumar, N-Substituted Pyrido-1,4-Oxazin-3-Ones Induce Apoptosis of Hepatocellular Carcinoma Cells by Targeting NF- $\kappa$ B Signaling Pathway, *Front. Pharmacol.* 9 (2018) 1125.
- [15] A.W.L. Chua, H.S. Hay, P. Rajendran, M.K. Shanmugam, F. Li, P. Bist, E.S.C. Koay, L. H.K. Lim, A.P. Kumar, G. Sethi, Butein downregulates chemokine receptor CXCR4 expression and function through suppression of NF- $\kappa$ B activation in breast and pancreatic tumor cells, *Biochem. Pharmacol.* 80 (2010) 1553–1562.

- [16] K.A. Manu, M.K. Shanmugam, L. Ramachandran, F. Li, C.W. Fong, A.P. Kumar, P. Tan, G. Sethi, First evidence that gamma-tocotrienol inhibits the growth of human gastric cancer and chemosensitizes it to capecitabine in a xenograft mouse model through the modulation of NF-kappaB pathway, *Clin. Cancer Res.* 18 (2012) 2220–2229.
- [17] H.K. Keerthy, C.D. Mohan, K. Sivaraman Siveen, J.E. Fuchs, S. Rangappa, M.S. Sundaram, F. Li, K.S. Girish, G. Sethi, A. Basappa, K. Bender, S. Rangappa, Novel synthetic biscoumarins target tumor necrosis factor-alpha in hepatocellular carcinoma in vitro and in vivo, *J. Biol. Chem.* 289 (2014) 31879–31890.
- [18] E.M. Shin, H.S. Hay, M.H. Lee, J.N. Goh, T.Z. Tan, Y.P. Sen, S.W. Lim, E.M. Yousef, H. T. Ong, A.A. Thike, X. Kong, Z. Wu, E. Mendoza, W. Sun, M. Salto-Tellez, C.T. Lim, P. E. Lobie, Y.P. Lim, C.T. Yap, Q. Zeng, G. Sethi, M.B. Lee, P. Tan, B.C. Goh, L.D. Miller, J.P. Thiery, T. Zhu, L. Gaboury, P.H. Tan, K.M. Hui, G.W. Yip, S. Miyamoto, A.P. Kumar, V. Tergaonkar, DEAD-box helicase DP103 defines metastatic potential of human breast cancers, *J. Clin. Invest.* 124 (2014) 3807–3824.
- [19] K.A. Manu, M.K. Shanmugam, F. Li, L. Chen, K.S. Siveen, K.S. Ahn, A.P. Kumar, G. Sethi, Simvastatin sensitizes human gastric cancer xenograft in nude mice to capecitabine by suppressing nuclear factor-kappa B-regulated gene products, *J. Mol. Med.* 92 (2014) 267–276.
- [20] G. Sethi, K.S. Ahn, M.M. Chaturvedi, B.B. Aggarwal, Epidermal growth factor (EGF) activates nuclear factor-kappaB through IkkappaBalpha kinase-independent but EGF receptor-kinase dependent tyrosine 42 phosphorylation of IkkappaBalpha, *Oncogene.* 26 (2007) 7324–7332.
- [21] M. Neelgundmath, K.R. Dinesh, C.D. Mohan, F. Li, X. Dai, K.S. Siveen, S. Paricharak, D.J. Mason, J.E. Fuchs, G. Sethi, A. Bender, K.S. Rangappa, O. Kotresh, Basappa, Novel synthetic coumarins that targets NF-kappaB in Hepatocellular carcinoma, *Bioorg. Med. Chem. Lett.* 25 (2015) 893–897.
- [22] A. Dey, E. Wong, N. Kua, H.L. Teo, V. Tergaonkar, D. Lane, Hexamethylene bisacetamide (HMBA) simultaneously targets AKT and MAPK pathway and represses NF kappaB activity: implications for cancer therapy, *Cell Cycle* 7 (2008) 3759–3767.
- [23] E.Z. Chai, K.S. Siveen, M.K. Shanmugam, F. Arfuso, G. Sethi, Analysis of the intricate relationship between chronic inflammation and cancer, *Biochem. J.* 468 (2015) 1–15.
- [24] C.D. Mohan, S. Hari, H.D. Preetham, S. Rangappa, U. Barash, N. Ilan, S.C. Nayak, V.K. Gupta, I. Basappa, K. Vlodavsky, S. Rangappa, Targeting heparanase in Cancer: inhibition by synthetic, chemically modified, and natural compounds, *iScience.* 15 (2019) 360–390.
- [25] M.H. Park, J.T. Hong, Roles of NF- $\kappa$ B in Cancer and inflammatory diseases and their therapeutic approaches, *Cells.* 5 (2016) 15.
- [26] P.S. Son, S.A. Park, H.K. Na, D.M. Jue, S. Kim, Y.J. Surh, Piceatannol, a catechol-type polyphenol, inhibits phorbol ester-induced NF- $\kappa$ B activation and cyclooxygenase-2 expression in human breast epithelial cells: cysteine 179 of IKK( $\beta$ ) as a potential target, *Carcinogenesis.* 31 (2010) 1442–1449.
- [27] F. Li, G. Sethi, Targeting transcription factor NF-kappaB to overcome chemoresistance and radioresistance in cancer therapy, *Biochim. Biophys. Acta* 1805 (2010) 167–180.
- [28] X. Xiao, G. Yang, P. Bai, S. Gui, T.M.B. Nguyen, I. Mercado-Urbe, M. Yang, J. Zou, Q. Li, J. Xiao, B. Chang, G. Liu, H. Wang, J. Liu, Inhibition of nuclear factor-kappa B enhances the tumor growth of ovarian cancer cell line derived from a low-grade papillary serous carcinoma in p53-independent pathway, *BMC Cancer* 16 (2016) 582.
- [29] G. Sethi, B. Sung, B.B. Aggarwal, Nuclear factor-kappaB activation: from bench to bedside, *Exp. Biol. Med.* (Maywood) 233 (2008) 21–31.
- [30] A. Subramaniam, M.K. Shanmugam, T.H. Ong, F. Li, E. Perumal, L. Chen, S. Vali, T. Abbasi, S. Kapoor, K.S. Ahn, A.P. Kumar, K.M. Hui, G. Sethi, Emodin inhibits growth and induces apoptosis in an orthotopic hepatocellular carcinoma model by blocking activation of STAT3, *Br. J. Pharmacol.* 170 (2013) 807–821.
- [31] D.I. Tai, S.L. Tsai, Y.H. Chang, S.N. Huang, T.C. Chen, K.S. Chang, Y.F. Liaw, Constitutive activation of nuclear factor kappaB in hepatocellular carcinoma, *Cancer.* 89 (2000) 2274–2281.
- [32] W. Li, D. Tan, M.J. Zenali, R.E. Brown, Constitutive activation of nuclear factor-kappa B (NF- $\kappa$ B) signaling pathway in fibrolamellar hepatocellular carcinoma, *Int. J. Clin. Exp. Pathol.* 3 (2009) 238–243.
- [33] L. Qiao, H. Zhang, J. Yu, R. Francisco, P. Dent, M.P.A. Ebert, C. Röcken, D.G. Farrell, Constitutive activation of NF- $\kappa$ B in human hepatocellular carcinoma: evidence of a cytoprotective role, *Hum. Gene Ther.* 17 (2006) 280–290.
- [34] S. Ananthula, P. Parajuli, F.A. Behery, A.Y. Alayoubi, S. Nazzal, K. El Sayed, P.W. Sylvester, -Tocotrienol oxazine derivative antagonizes mammary tumor cell compensatory response to CoCl<sub>2</sub>-Induced hypoxia, *Biomed Res. Int.* 2014 (2014) 13.
- [35] H. Bharathkumar, C.D. Mohan, S. Rangappa, T. Kang, H.K. Keerthy, J.E. Fuchs, N. H. Kwon, A. Bender, S. Kim, K. Basappa, S. Rangappa, Screening of quinoline, 1,3-benzoxazine, and 1,3-oxazine-based small molecules against isolated methionyl-tRNA synthetase and A549 and HCT116 cancer cells including an in silico binding mode analysis, *Org. Biomol. Chem.* 13 (2015) 9381–9387.
- [36] C.D. Mohan, H. Bharathkumar, K.C. Bulusu, V. Pandey, S. Rangappa, J.E. Fuchs, M.K. Shanmugam, X. Dai, F. Li, A. Deivasigamani, K.M. Hui, A.P. Kumar, P.E. Lobie, A. Bender, G. Basappa, K. Sethi, S. Rangappa, Development of a novel azaspirane that targets the Janus kinase-signal transducer and activator of transcription (STAT) pathway in hepatocellular carcinoma in vitro and in vivo, *J. Biol. Chem.* 289 (2014) 34296–34307.
- [37] A.C. Nirvanappa, C.D. Mohan, S. Rangappa, H. Ananda, A.Y. Sukhorukov, M.K. Shanmugam, M.S. Sundaram, S.C. Nayaka, K.S. Girish, A. Chinnthambi, M.E. Zayed, S.A. Alharbi, G. Sethi, K. Basappa, S. Rangappa, Novel synthetic oxazines target NF-kappaB in Colon Cancer In vitro and inflammatory bowel disease in vivo, *PLoS One* 11 (2016)e0163209.
- [38] V. Srinivas, C.D. Mohan, C.P. Baburajeev, S. Rangappa, S. Jagadish, J.E. Fuchs, A.Y. Sukhorukov, D.J. Chandra, K.S. Mason, S. Kumar, M. Madegowda, A. Bender, K. Basappa, S. Rangappa, Synthesis and characterization of novel oxazines and demonstration that they specifically target cyclooxygenase 2, *Bioorg. Med. Chem. Lett.* 25 (2015) 2931–2936.
- [39] N.B. Sulaiman, C.D. Mohan, S. Basappa, V. Pandey, S. Rangappa, H. Bharathkumar, A.P. Kumar, P.E. Lobie, K.S. Rangappa, An azaspirane derivative suppresses growth and induces apoptosis of ER-positive and ER-negative breast cancer cells through the modulation of JAK2/STAT3 signaling pathway, *Int. J. Oncol.* 49 (2016) 1221–1229.
- [40] F. Uzma, C.D. Mohan, A. Hashem, N.M. Konappa, S. Rangappa, P.V. Kamath, B.P. Singh, V. Mudili, V.K. Gupta, C.N. Siddaiah, S. Chowdappa, A.A. Alqarawi, E.F. Abd Allah, Endophytic fungi-alternative sources of cytotoxic compounds: a review, *Front. Pharmacol.* 9 (2018) 309.
- [41] S. Ananthula, P. Parajuli, F.A. Behery, A.Y. Alayoubi, K.A. El Sayed, S. Nazzal, P.W. Sylvester, Oxazine derivatives of gamma- and delta-tocotrienol display enhanced anticancer activity in vivo, *Anticancer Res.* 34 (2014) 2715–2726.
- [42] N. Ansari, F. Khodaghali, M. Amini, F. Shaerzadeh, Attenuation of LPS-induced apoptosis in NGF-differentiated PC12 cells via NF-kappaB pathway and regulation of cellular redox status by an oxazine derivative, *Biochimie.* 93 (2011) 899–908.
- [43] K.S. Rakesh, S. Jagadish, T.R. Swaroop, C.D. Mohan, N. Ashwini, K.B. Harsha, F. Zameer, K.S. Girish, K.S. Rangappa, Anti-cancer activity of 2,4-Disubstituted thiophene derivatives: dual inhibitors of Lipoxigenase and cyclooxygenase, *Med. Chem.* 11 (2015) 462–472.
- [44] N.C. Anilkumar, M.S. Sundaram, C.D. Mohan, S. Rangappa, K.C. Bulusu, J.E. Fuchs, K.S. Girish, A. Bender, K. Basappa, S. Rangappa, A One Pot Synthesis of Novel Bioactive Tri-Substitute-Condensed-Imidazopyridines that Targets Snake Venom Phospholipase A2, *PLoS One* 10 (2015)e0131896.
- [45] N. Ashwini, M. Garg, C.D. Mohan, J.E. Fuchs, S. Rangappa, S. Anusha, T.R. Swaroop, K.S. Rakesh, D. Kanojia, V. Madan, A. Bender, H.P. Koefler, K. Basappa, S. Rangappa, Synthesis of 1,2-benzisoxazole tethered 1,2,3-triazoles that exhibit anticancer activity in acute myeloid leukemia cell lines by inhibiting histone deacetylases, and inducing p21 and tubulin acetylation, *Bioorg. Med. Chem.* 23 (2015) 6157–6165.
- [46] C.D. Mohan, V. Srinivasa, S. Rangappa, L. Mervin, S. Mohan, S. Paricharak, S. Baday, F. Li, M.K. Shanmugam, A. Chinnthambi, M.E. Zayed, S.A. Alharbi, A. Bender, G. Sethi, K. Basappa, S. Rangappa, Trisubstituted-imidazoles induce apoptosis in human breast Cancer cells by targeting the oncogenic PI3K/Akt/mTOR signaling pathway, *PLoS One* 11 (2016)e0153155.
- [47] M. Gilandoust, K.B. Harsha, C.D. Mohan, A.R. Raquib, C. Rangappa, V. Pandey, P. E. Lobie, K. Basappa, S. Rangappa, Synthesis, characterization and cytotoxicity studies of 1,2,3-triazoles and 1,2,4-triazolo [1,5-a] pyrimidines in human breast cancer cells, *Bioorg. Med. Chem. Lett.* 28 (2018) 2314–2319.
- [48] A. Sebastian, V. Pandey, C.D. Mohan, Y.T. Chia, S. Rangappa, J. Mathai, C.P. Baburajeev, S. Paricharak, L.H. Mervin, K.C. Bulusu, J.E. Fuchs, A. Bender, S. Yamada, P.E. Basappa, K. Lobie, S. Rangappa, Novel adamantanyl-based thiadiazolyl pyrazoles targeting EGFR in triple-negative breast Cancer, *ACS Omega* 1 (2016) 1412–1424.
- [49] A.Y. Sukhorukov, A.C. Nirvanappa, J. Swamy, S.L. Ioffe, S. Nanjunda Swamy, K.S. Basappa, Rangappa, Synthesis and characterization of novel 1,2-oxazine-based small molecules that targets acetylcholinesterase, *Bioorg. Med. Chem. Lett.* 24 (2014) 3618–3621.
- [50] S. Anusha, B.S. Anandakumar, C.D. Mohan, G.P. Nagabhushana, B.S. Priya, K.S. Rangappa, C.G.T. Basappa, Preparation and use of combustion-derived Bi2O3 for the synthesis of heterocycles with anti-cancer properties by Suzuki-coupling reactions, *RSC Adv.* 4 (2014) 52181–52188.
- [51] S. Anusha, C.D. Mohan, H. Ananda, C.P. Baburajeev, S. Rangappa, J. Mathai, J.E. Fuchs, F. Li, M.K. Shanmugam, A. Bender, G. Sethi, K. Basappa, S. Rangappa, Adamantyl-tethered-biphenylic compounds induce apoptosis in cancer cells by targeting Bcl homologs, *Bioorg. Med. Chem. Lett.* 26 (2016) 1056–1060.
- [52] C.C. Woo, A. Hsu, A.P. Kumar, G. Sethi, K.H.B. Tan, Thymoquinone inhibits tumor growth and induces apoptosis in a breast Cancer xenograft mouse model: the role of p38 MAPK and ROS, *PLoS One* 8 (2013)e75356.
- [53] R. Roopashree, C.D. Mohan, T.R. Swaroop, S. Jagadish, B. Raghava, K.S. Balaji, S. Jayarama, K.S. Basappa, Rangappa, Novel synthetic bisbenzimidazole that targets angiogenesis in Ehrlich ascites carcinoma bearing mice, *Bioorg. Med. Chem. Lett.* 25 (2015) 2589–2593.
- [54] C.P. Baburajeev, C. Dhananjaya Mohan, H. Ananda, S. Rangappa, J.E. Fuchs, S. Jagadish, K. Sivaraman Siveen, A. Chinnthambi, S. Ali Alharbi, M.E. Zayed, J. Zhang, F. Li, G. Sethi, K.S. Girish, A. Bender, K. Basappa, S. Rangappa, Development of novel triazolo-thiadiazoles from heterogeneous “Green” catalysis as protein tyrosine phosphatase 1B inhibitors, *Sci. Rep.* 5 (2015) 14195.
- [55] K.N. Nandees, H.A. Swarup, N.C. Sandhya, C.D. Mohan, C.S. Pavan Kumar, M.N. Kumara, K. Mantelingu, S. Ananda, K.S. Rangappa, Synthesis and antiproliferative efficiency of novel bis(imidazol-1-yl)vinyl-1,2,4-oxadiazoles, *New J. Chem.* 40 (2016) 2823–2828.
- [56] S.M. Tan, F. Li, P. Rajendran, A.P. Kumar, K.M. Hui, G. Sethi, Identification of beta-escin as a novel inhibitor of signal transducer and activator of transcription 3/Janus-activated kinase 2 signaling pathway that suppresses proliferation and induces apoptosis in human hepatocellular carcinoma cells, *J. Pharmacol. Exp. Ther.* 334 (2010) 285–293.

- [57] H.K. Keerthy, M. Garg, C.D. Mohan, V. Madan, D. Kanojia, R. Shobith, S. Nanjundaswamy, D.J. Mason, A. Bender, K.S. Basappa, H.P. Rangappa, Koeffler, Synthesis and characterization of novel 2-amino-chromene-nitriles that target Bcl-2 in acute myeloid leukemia cell lines, *PLoS One* 9 (2014) e107118.
- [58] V. Pandey, B. Wang, C.D. Mohan, A.R. Raquib, S. Rangappa, V. Srinivasa, J.E. Fuchs, K.S. Girish, T. Zhu, A. Bender, L. Ma, Z. Yin, K. Basappa, S. Rangappa, P.E. Lobie, Discovery of a small-molecule inhibitor of specific serine residue BAD phosphorylation, *Proc. Natl. Acad. Sci. U S A* 115 (2018) E10505–e10514.
- [59] K.S. Rakesh, S. Jagadish, K.S. Balaji, F. Zameer, T.R. Swaroop, C.D. Mohan, S. Jayarama, K.S. Rangappa, 3,5-disubstituted isoxazole derivatives: potential inhibitors of inflammation and Cancer, *Inflammation*. 39 (2016) 269–280.
- [60] S.S. Singh, W.N. Yap, F. Arfuso, S. Kar, C. Wang, W. Cai, A.M. Dharmarajan, G. Sethi, A.P. Kumar, Targeting the PI3K/Akt signaling pathway in gastric carcinoma: A reality for personalized medicine? *World J. Gastroenterol.* 21 (2015) 12261–12273.
- [61] K.S. Oh, S. Lee, J.K. Choi, B.H. Lee, Identification of novel scaffolds for IκB kinase beta inhibitor via a high-throughput screening TR-FRET assay, *Comb. Chem. High T. Scr.* 13 (2010) 790–797.
- [62] G. Lyss, A. Knorre, T.J. Schmidt, H.L. Pahl, I. Merfort, The anti-inflammatory sesquiterpene lactone helenalin inhibits the transcription factor NF-κB by directly targeting p65, *J. Biol. Chem.* 273 (1998) 33508–33516.
- [63] R. Chandramohanadas, B. Basappa, K. Russell, Y.H. Liew, A. Yau, M. Chong, K. Liu, R. Gunalan, L. Raman, F. Renia, S.G. Nosten, M. Shochat, R. Dao, S. Sasisekharan, P. Suresh, Preiser, Small molecule targeting malaria merozoite surface protein-1 (MSP-1) prevents host invasion of divergent plasmodial species, *J. Infect. Dis.* 210 (2014) 1616–1626.
- [64] S.G. Mansouri, H. Zali-Boeini, K. Zomorodian, B. Khalvati, R.H. Pargali, A. Dehshahri, H.A. Rudbari, M. Sahihi, Z. Chavoshpour, Synthesis of novel naphtho[1,2-e][1,3]oxazines bearing an arylsulfonamide moiety and their anticancer and antifungal activity evaluations, *Arab. J. Chem.* 13 (2020) 1271–1282.
- [65] D. Plesca, S. Mazumder, A. Almasan, DNA damage response and apoptosis, *Method. Enzymol.* 446 (2008) 107–122.
- [66] Y. Xia, S. Shen, I.M. Verma, NF-κB, an active player in human cancers, *Cancer Immunol. Res.* 2 (2014) 823–830.
- [67] S.K. Manna, R.S. Aggarwal, G. Sethi, B.B. Aggarwal, G.T. Ramesh, Morin (3,5,7,2',4'-Pentahydroxyflavone) abolishes nuclear factor-kappaB activation induced by various carcinogens and inflammatory stimuli, leading to suppression of nuclear factor-kappaB-regulated gene expression and up-regulation of apoptosis, *Clin. Cancer Res.* 13 (2007) 2290–2297.
- [68] M. Sawhney, N. Rohatgi, J. Kaur, S. Shishodia, G. Sethi, S.D. Gupta, S.V. Deo, N.K. Shukla, B.B. Aggarwal, R. Ralhan, Expression of NF-κB parallels COX-2 expression in oral precancer and cancer: association with smokeless tobacco, *Int. J. Cancer* 120 (2007) 2545–2556.
- [69] K.S. Ahn, G. Sethi, M.M. Chaturvedi, B.B. Aggarwal, Simvastatin, 3-hydroxy-3-methylglutaryl coenzyme A reductase inhibitor, suppresses osteoclastogenesis induced by receptor activator of nuclear factor-kappaB ligand through modulation of NF-κB pathway, *Int. J. Cancer* 123 (2008) 1733–1740.
- [70] K.S. Ahn, G. Sethi, B.B. Aggarwal, Reversal of chemoresistance and enhancement of apoptosis by statins through down-regulation of the NF-κB pathway, *Biochem. Pharmacol.* 75 (2008) 907–913.
- [71] G. Sethi, K.S. Ahn, B. Sung, B.B. Aggarwal, Pinitol targets nuclear factor-kappaB activation pathway leading to inhibition of gene products associated with proliferation, apoptosis, invasion, and angiogenesis, *Mol. Cancer Ther.* 7 (2008) 1604–1614.
- [72] D.K. Sarkar, D. Jana, P.S. Patil, K.S. Chaudhari, B.K. Chattopadhyay, B.R. Chikkala, S. Mandal, P. Chowdhary, Role of NF-κB as a prognostic marker in breast Cancer : a pilot study in indian patients, *Indian J. Surg. Oncol.* 4 (2013) 242–247.
- [73] L. Gu, Z. Wang, J. Zuo, H. Li, L. Zha, Prognostic significance of NF-κB expression in non-small cell lung cancer: a meta-analysis, *PLoS One* 13 (2018) e0198223.
- [74] K.S. Ahn, G. Sethi, A.K. Jain, A.K. Jaiswal, B.B. Aggarwal, Genetic deletion of NAD (P)H:quinone oxidoreductase 1 abrogates activation of nuclear factor-kappaB, IκBα kinase, c-Jun N-terminal kinase, Akt, p38, and p44/42 mitogen-activated protein kinases and potentiates apoptosis, *J. Biol. Chem.* 281 (2006) 19798–19808.